Parasitology

cambridge.org/par

Invasive *Pseudosuccinea columella* enters the transmission cycle of an amphistome parasite infecting African buffalo

Emilie Goossens[1,2,3], Ruben Schols[2,4], Aspire Mudavanhu[5,6], Tawanda Manyangadze[7,8], Joachim Mariën[3,9], Maarten P. M. Vanhove[1,10] and Tine Huyse[2,5]

[1]Research Group Zoology: Biodiversity & Toxicology, Center for Environmental Sciences, Hasselt University, Diepenbeek, Belgium; [2]Department of Biology, Royal Museum for Central Africa, Tervuren, Belgium; [3]Virus Ecology Unit, Department of Biomedical Sciences, Institute of Tropical Medicine, Antwerp, Belgium; [4]Laboratory of Aquatic Biology, Microbiome EcoEvo Unit, KU Leuven - Kulak Kortrijk Campus, Kortrijk, Belgium; [5]Laboratory of Animal Ecology, Global Change and Sustainable Development, KU Leuven, Leuven, Belgium; [6]Department of Biological Sciences, Bindura University of Science Education, Bindura, Zimbabwe; [7]Geosciences Department, Bindura University of Science Education, Bindura, Zimbabwe; [8]School of Medicine, College of Health Sciences, University of KwaZulu-Natal, Durban, South Africa; [9]Evolutionary Ecology group, University of Antwerp, Antwerp, Belgium and [10]Freshwater Biology, Operational Directorate Natural Environment, Royal Belgian Institute of Natural Sciences, Brussels, Belgium

Research Article

Cite this article: Goossens E, Schols R, Mudavanhu A, Manyangadze T, Mariën J, Vanhove M, Huyse T (2026) Invasive *Pseudosuccinea columella* enters the transmission cycle of an amphistome parasite infecting African buffalo. *Parasitology*, 1–18. https://doi.org/10.1017/S0031182026102728

Received: 1 March 2026 UTC
Revised: 3 August 2026 UTC
Accepted: 5 August 2026 UTC

Keywords:
anthropogenic and environmental stress; fascioliasis; helminth parasites; invasive snails; paramphistomosis; *Syncerus caffer*; wildlife disease ecology; xenomonitoring

Corresponding author: Emilie Goossens; Email: emilie.goossens@uhasselt.be

Abstract

Parasite transmission and disease outcomes in African wildlife are increasingly shaped by anthropogenic environmental change, yet empirical data linking parasites, intermediate hosts and wildlife health remain scarce. Following an unexplained increase in mortality among wild ruminants at a Zimbabwean conservancy, we investigated the diversity, transmission and potential health relevance of snail-borne trematodes within this managed wildlife conservancy. We combined a post-mortem examination of an African buffalo (*Syncerus caffer*), standardized freshwater snail surveys, cercarial shedding experiments, DNA-based screening in snails, and morphological and molecular analyses of snails and parasites. The buffalo was infected with the liver fluke *Fasciola gigantica* and an amphistome identified as *Calicophoron* aff. *microbothrium*. Snail surveys revealed 4 gastropod taxa: invasive *Physella acuta* and *Pseudosuccinea columella*, and native *Radix natalensis* and a *Lentorbis*-like planorbid. The latter 3 species hosted trematode infections. Molecular screening linked *C.* aff. *microbothrium* infections in the buffalo to a shedding *P. columella*, providing the first evidence that this invasive snail is a competent intermediate host for this amphistome. No snails were found infected with *F. gigantica*. Additional trematodes detected in snails included *Plagiorchis maculosus, Plagiorchis* sp., *Echinostoma* sp., and another species of the order Plagiorchiida. The presence of *P. columella* as a competent intermediate host, combined with its known role in *Fasciola* transmission in Africa, highlights the potential for parasite spillback and elevated disease transmission. Our findings underscore the value of integrated approaches and emphasize persistent taxonomic and ecological knowledge gaps that limit understanding of trematode-driven disease dynamics in African wildlife.

Introduction

Parasites form a critical component of resilient ecosystems, providing important ecosystem services that underscore the need for their conservation (Carlson et al., 2020). However, some parasites pose significant threats to human health, livestock production and wildlife conservation (Johansen et al., 2015; Mehmood et al., 2017; De Oliveira et al., 2024). Furthermore, anthropogenic pressures can drastically alter parasite transmission, compromising both human and animal health (Sow et al., 2002; Jones et al., 2013; Thompson, 2013; Gottdenker et al., 2014) and shifting the balance in parasite-mediated competition (Price et al., 1986; Schall, 1992; Tompkins et al., 2003), whereby both effects often shape community structure, biodiversity and therefore conservation efforts. Together, these contrasting roles highlight parasitism as a complex and context-dependent process with important implications for wildlife conservation and management.

The ultimate effect of parasites on host health is often dependent on co-infections with other pathogens, environmental stressors, and anthropogenic pressures. For instance, parasite-mediated immune modulation or tissue damage can facilitate concomitant or secondary infections, which ultimately drive disease severity and host mortality (Allen and Wynn, 2011;

Demann and Wegner, 2019). Environmental pressures, such as temperature fluctuations and resource limitation, can additionally influence disease outcomes (Vicente-Santos et al., 2023). Such multifactorial dynamics have become increasingly relevant in the Anthropocene, where anthropogenic stressors, including habitat alteration, global warming, and pollution, are reshaping aquatic ecosystems and modulating host–parasite relationships, which can result in elevated host morbidity or mortality (Marcogliese and Pietrock, 2011; Schols et al., 2021). Trematodes exemplify this complexity: as parasites with intricate, multi-host life cycles, they are highly sensitive to environmental change, with their transmission dynamics often responding non-linearly to temperature shifts and pollution (Sures et al., 2023).

Artificial water bodies, such as man-made dams, are particularly prone to environmental and anthropogenic modifications, including altered physicochemical conditions and the introduction of invasive species. These can consequently intensify trematode transmission and disease risk (Morley, 2007; Telfer and Bown, 2012; Carolus et al., 2019). For instance, the creation of the artificial Lake Kariba in Zimbabwe facilitated both the spillback and potential spillover of trematode infections in large herbivores such as the hippopotamus through a cascade of biological invasions (Carolus et al., 2019; Schols et al., 2021). Although comparable empirical data for terrestrial megafauna remain limited, anthropogenic modifications to the environment are increasingly linked to enhanced parasite transmission and disease burden in wildlife (Brearley et al., 2013), with examples from elephants and primates (Vítovec et al., 1984; Gillespie and Chapman, 2008). Therefore, understanding environmental drivers of disease burden and transmission dynamics is critical for predicting disease outcomes and developing effective conservation and management strategies in a rapidly changing world.

Fasciolosis, also known as liver rot, is a trematode-induced disease that is particularly sensitive to environmental modifications and changes in freshwater habitats (Alba et al., 2021). It is caused by *Fasciola* species, of which 3 are linked to animal disease in Africa: *Fasciola hepatica* (Linnaeus, 1758), *Fasciola gigantica* (Cobbold, 1856), and *Fasciola nyanzae* (Leiper, 1910) (McCully et al., 1967; Malatji et al., 2020). They infect the liver of livestock and wild ruminants, causing anaemia, weight loss, lesions and fibrosis in the liver, haemorrhage and ultimately death (Behm and Sangster, 1999). Most studies focus on livestock due to the severe economic burden (Mehmood et al., 2017), whereas infections in wildlife remain severely neglected (Malatji et al., 2020; Namirembe et al., 2024). In Southern Africa, transmission occurs via freshwater snails belonging to Lymnaeidae, mostly by *Radix natalensis* (Krauss, 1848), *Galba* spp. (Schrank, 1803) (Mahulu et al., 2019) and the invasive snail *Pseudosuccinea columella* (Say, 1817). Upon release from the freshwater snail host, cercariae encyst on aquatic vegetation, after which they are ingested by the final host (Malatji et al., 2020; Nukeri et al., 2022).

Amphistomes, or stomach flukes, represent another important group of trematodes infecting ruminants. Members of Paramphistomoidea (Fischoeder, 1901) cause paramphistomosis or amphistomiasis when infecting the rumen and reticulum of ruminants. The adults generally are of low pathogenicity, but immature stages cause severe clinical disease when they migrate from the small intestine to the rumen, leading to weight loss, anaemia, decreased milk production, and even death (Elelu and Eisler, 2018; Pfukenyi and Mukaratirwa, 2018). Similar to fasciolosis, the burden of amphistomiasis on wildlife remains severely understudied, despite the disease's wide geographic distribution and potentially great impact on animal health (Sibula et al., 2024b). The most widespread species, possibly a species complex (Laidemitt et al., 2019), causing amphistomiasis in Africa is *Calicophoron microbothrium* (Fischoeder, 1901), whose reported host snails are mostly *Bulinus* species (Pfukenyi and Mukaratirwa, 2018; Sibula et al., 2024b), although recently a natural infection in the non-native *Melanoides tuberculata* (O. F. Müller, 1774) has been reported (Sibula et al., 2024a). Similar to liver flukes, amphistomes encyst on vegetation to reach their final host through ingestion (Ghatani and Tandon, 2024).

Both liver and stomach flukes infect African buffalo (*Syncerus caffer* Sparrman, 1779) (Bengis et al., 2023; Sibula et al., 2024b). This species is the largest African bovid and occurs in diverse ecosystems across the continent, from rainforests to savannas. It is water-dependent and lives in complex social herds (Taylor et al., 2023). As a result of habitat loss, poaching, increasing droughts and diseases, the species' conservation status has been updated from 'least concern' to 'nearly threatened' (IUCN SSC Antelope Specialist Group 2019), despite regional disparities (Cornelis et al., 2023). Besides conservation, the African buffalo is also a species of interest from a One Health perspective. Buffaloes and cattle both belong to the tribe Bovini and therefore have many common pathogens that cause severe disease in cattle, such as bovine tuberculosis, brucellosis and several trematodiases (Le Roex et al., 2016; Pfukenyi and Mukaratirwa, 2018; Bengis et al., 2023). The latter can cause mortality in *S. caffer* either directly or indirectly through interactions with other pathogens (Ezenwa and Jolles, 2015; Woodburn et al., 2021).

In the early cold season (June–July 2023), 26 wild ruminants died at the Imire Rhino & Wildlife Conservancy in Zimbabwe, a sharp contrast to the limited animal losses in 2022. Especially the loss of 4 young African buffaloes caused concern to the management team. Earlier post-mortem examinations of 2 greater Kudus (*Tragelaphus strepsiceros* Pallas, 1766) by veterinarians listed snail-borne parasites as one of the potential causes of these unexplained deaths. Therefore, a snail survey combined with a post-mortem examination of a culled buffalo was conducted to identify and monitor trematode infections that potentially contributed to the observed increase in buffalo mortality.

Materials and methods

Study area

A snail and trematode survey was conducted in Imire Rhino and Wildlife Conservancy (referred to as Imire) during the cold dry season (winter) in August 2023. Imire is located in the northern part of Hwedza District, Zimbabwe, bordering Marondera District. The region experiences a temperate highland tropical climate, characterised by distinct dry and rainy seasons, with a mean annual precipitation of approximately 675 mm and an annual average temperature of 21.5 °C. Imire consists of 3 fenced conservation areas and an adjacent zone dedicated to irrigated tobacco farming, a land-use practice that is widespread in this region of Zimbabwe. To secure water supplies for irrigation and wildlife, particularly under increasing climatic variability, several rivers and creeks within Imire have been dammed, resulting in multiple artificial water bodies. One artificial reservoir (Site W) was only created in 2018 and is permanently topped up with borehole water. Sampling was conducted in the Lodge section, the northernmost conservation section, which directly borders the agricultural area (Figure 1). This section encompasses the full range of the resident buffalo herd,

https://doi.org/10.1017/S0031182026102728

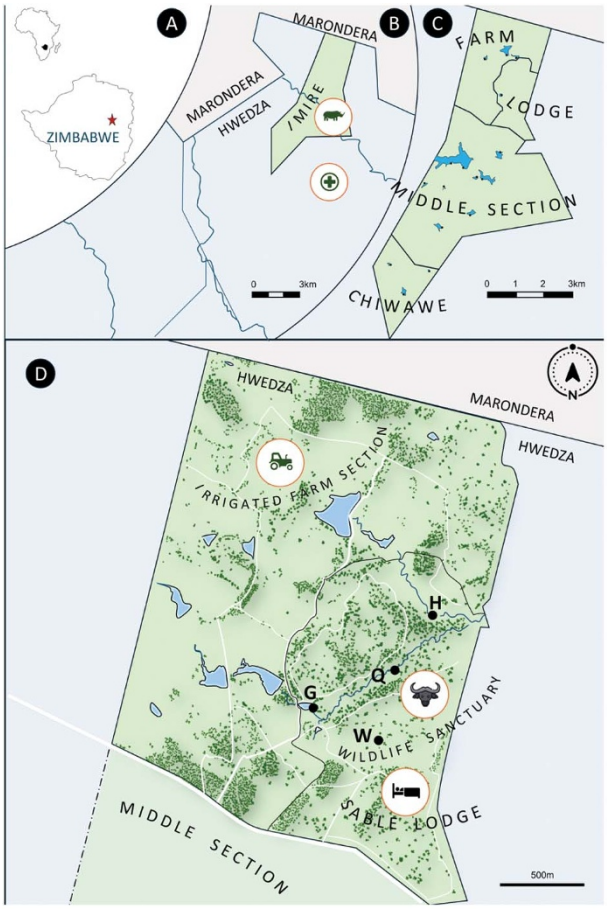

Figure 1. Study area and sampling locations at Imire Rhino and Wildlife Conservancy, Hwedza District, Zimbabwe. (A) Location of the study area within Zimbabwe, Southern Africa. (B) Position of Imire within Hwedza District. (C) Spatial partitioning of Imire into 4 management sections from south to north: Chiwawe, Middle section, Farm section and Lodge section. (D) Detailed map of the Lodge section showing freshwater bodies sampled for snail intermediate hosts, indicated as black dots with their respective site letter codes.

as well as other large mammals, including elephant, wildebeest, antelope and baboons. Accordingly, all water bodies within this section (1 natural creek and 3 man-made dams) were surveyed for freshwater snails.

Trematode recovery from buffalo and snail hosts

A post-mortem examination was conducted on 18 August 2023 at 10:30 on a female African buffalo, estimated 8–10 years old, approximately 1 h after being culled in close proximity to Site G (Mermaid's dam). The buffalo herd was scheduled for their annual fluke treatment the following week, typically administered immediately before or after the winter or rainy season. Treatment consists of Flukazole C (Virbac, Triclabendazole 12% mass/volume and Oxfendazole 4.53% mass/volume) drenched cubes for oral intake. The herd had been treated with an undetermined insecticide against ticks. Conservation managers reported that the culled buffalo had exhibited markedly poor health during the week preceding culling, including difficulty remaining upright. On the day of culling, the animal was unable to stand and was found recumbent near the water's edge at Site G. It allowed close human approach and was euthanized with a shot to the temple. During the necropsy, general health indicators, including body mass, coat condition, body fat reserves, organ condition and the presence of cysts or lesions, were assessed. The liver, stomach compartments and mesenteric veins were inspected for the presence of trematode parasites. The liver was screened for liver flukes by opening and inspecting the bile ducts and by sectioning the liver tissue using a scalpel. All stomach compartments were opened, and the mucosal surfaces were visually inspected for the presence of stomach flukes. Finally, the mesenteric veins were screened for blood flukes by transillumination, i.e. holding a bright light behind the tissue to detect (moving) adult schistosomes. During collection in the field, live stomach flukes were first relaxed in 50 mL tubes containing warm saline solution (approximately 70 °C; 9 g NaCl per litre of borehole water) and fixed in 70% ethanol for morphological and subsequent molecular identification.

Freshwater snails were collected in a standardized way by 2 persons sampling for 30 min per site using scooping nets with a mesh size of 1 mm. Snails were transported alive to the field lab in ambient water, where they were identified to species or genus level using keys by Mandahl-Barth (1962), Brown (1994), and Appleton and Miranda (2015). Identification was additionally supported by previous morphological and molecular studies of snails at the same study sites (Mudavanhu et al., 2024a, 2024b). Snails were grouped per morphotype and stored in the dark overnight in multiwell plates filled with borehole water. Before sunrise, all wells were inspected using a stereomicroscope for the emergence of cercariae, which are the larval trematode stages, from the snails. At sunrise, shedding experiments started, whereby the release of cercariae was stimulated by exposing the snails to indirect sunlight at the windowsill combined with artificial lighting. All wells were checked for the emergence of cercariae using a stereomicroscope at 3 time points: at sunrise (06:30), before noon (08:00–10:00) and at the end of the shedding experiment in the late afternoon (15:00–17:00). As a consequence of these time frames, however, *C.* aff. *microbothrium* cercariae had already encysted on the surface of the plastic multiwell plates after shedding. Amphistome cercariae encyst on vegetation following release from their snail intermediate host in natural settings, and have been shown to encyst on various other biotic and abiotic surfaces, including plastic multiwell plates (LeSage and Fried, 2011). Therefore, subsequent analysis and reporting were based on the metacercarial form. Snails, cercariae and metacercariae were subsequently stored in 80% ethanol and transported to Belgium for molecular analysis.

Imaging

Imaging was performed for digital archiving and to document and assess diagnostic morphological traits of snails and trematode parasites. Adult parasites and snails were photographed using the focus-stacking technique described in Brecko et al. (2014) and Schols et al. (2021). Histological sections of the stomach flukes were digitized with a Leica DMLB using Objective Imaging through the Surveyor software (version 8.0.0.2) at 5× magnification and saved as bitmap files with ×2 scaling to reduce file size. Key diagnostic features, including the genital pore, pharynx, and acetabulum, were imaged at 10× magnification. Multiple images of each specimen were captured at successive focal depths and subsequently merged into a single high-depth-of-field image using Zerene Stacker and the Pmax option (version 1.04 Build T2022-04-21-0715). Cercariae and metacercariae were washed in water, isolated on microscopic slides, and photographed using a BMS camera (model number: XFCAM1080PHD) and associated BMS Pix3 software (version

https://doi.org/10.1017/S0031182026102728

4.12.24621.20240204). Subsequently, cercarial types were morphologically classified according to Frandsen and Christensen (1984). Final image processing was performed in Adobe Photoshop (version 26.9.0) to remove background artefacts, add scale bars and assemble multiple orientations of individual specimens into a single figure. Morphometric measurements were obtained from images of 80% ethanol-fixed cercariae and metacercariae using ImageJ version 1.54f.

Morphological analysis of stomach flukes

Stomach flukes were morphologically identified based on median sagittal sections and scanning electron microscopy (SEM) following keys by Sey (1991) and Eduardo (1983). Median sagittal sections were made to examine the internal morphological traits of the collected stomach flukes. First, samples were submerged in 100% ethanol for 2 times 1 h. Next, they were incubated in 1:1 ethanol/butanol (1 h), 100% butanol (1 h), 100% butanol/paraffin (overnight) and 100% paraffin (4 h). After being embedded in paraffin, sections of 10 µm were cut with a Leica SM 2000R sliding microtome and collected on glass slides. Then the sections were dried on a warm plate and deparaffinized gradually to dH_2O by first washing them 3 times with xylene and subsequently in a descending series of ethanol: 100% absolute ethanol (2 times), followed by 96%, 90%, 75% and 50% ethanol each for 15 min. Finally, the sections were submerged in dH_2O for 10 min. The deparaffinized sections were then submerged in haematoxylin Ehrlich for 20 min and rinsed with tap water for 15 min. Next, they were stained with erythrosin 0.1% in dH_2O for 10 min. The sections were dehydrated in an ascending series of ethanol: 50%, 75%, 80% and 90% (a few seconds each), followed by 96% (10 min) and 100% absolute ethanol (2 times 15 min). Lastly, the sections were submerged in xylene for 2 times 20 min and mounted in Depex.

Two amphistome specimens were examined using SEM following Schols et al. (2025) to visualize the tegumental papillae and the genital pore region. The specimens were first dehydrated overnight in 100% ethanol, then submerged in 100% ether in a watch glass and incubated on a heating block (low heat) until dry. The resulting specimens were mounted on aluminium stubs using copper tape, coated with gold and examined using a JEOL JSM-6480LV SEM. The contrast of the resulting images was subsequently optimized in Adobe Photoshop.

Molecular analysis

Adult parasite DNA extraction

All 18 preserved liver flukes and a subset of 15 out of 35 stomach flukes (due to the more invasive tissue sampling in these smaller specimens) were selected for DNA extraction. A sterile scalpel was used to excise one-quarter to one-half of the acetabulum for 5 stomach flukes. However, since the acetabulum serves as a diagnostic morphological feature, a section from the dorsal tegument was taken from the remaining 10 stomach flukes. A tissue section of approximately 5 mm^2 was isolated from the lateral margin of liver flukes. Tissue samples were homogenized using a sterile scalpel and air-dried on sterile absorbent paper. The work surface, gloves and equipment were sterilized between specimens using DNA AWAY™ (Thermo Fisher™). Subsequently, genomic DNA extraction proceeded according to the manufacturer's guidelines using the proteinase *K*-based E.Z.N.A. Tissue DNA Kit (OMEGA Bio-tek). DNA was eluted in 2 elution steps using 75 µL of elution buffer. The eluate was subsequently diluted by adding 10 µL of the extract to 90 µL of sterile Milli-Q water (Rockland). From the remaining extract, 100 µL was dried on GenTegra™ DNA-Tubes for curation in the Royal Museum for Central Africa (RMCA) Biobank, while the remaining 40 µL was stored at −20 °C.

Snail DNA extraction

The snail tissue was carefully separated from the shell using thin tweezers and placed on absorbent paper to remove excess ethanol. The entire soft body was used for DNA extraction, while the shells were retained for curation in the RMCA collection. To prevent cross-contamination, all instruments were sterilized between specimens using ethanol and a flame. All collected snails were extracted, except for *Physella acuta*, for which a maximum of 50 individuals per site were extracted, as this invasive snail occurred in high numbers and is usually not infected with the targeted trematodes, while still allowing a sufficient sampling effort to detect trematode infections. DNA extraction was performed using the E.Z.N.A. Mollusk DNA Kit (OMEGA Bio-tek), following the manufacturer's protocol and using 2 elution steps, each with 75 µL elution buffer. Of the 150 µL eluate, 10 µL was added to 100 µL water to obtain a 1:10 dilution for downstream analysis. From the remaining extract, 100 µL was dried onto GenTegra™ DNA-Tubes for curation in the RMCA Biobank, and the remaining 40 µL was stored at −20 °C.

Cercariae DNA extraction

Four cercariae per shedding snail were transferred from their respective tube into a watch glass and washed in distilled water. Individual cercariae were then pipetted into wells of a PCR plate, each containing 5 µL of Ultrapure sterile water (Rockland). Next, a lysis buffer was prepared as in Zietara et al. (2000), and 10 µL of lysis buffer containing 1 µL of proteinase *K* was added to each well. The plate was gently swirled, briefly centrifuged and incubated at 65 °C for 25 min, followed by 96 °C for 10 min. Wells were then visually inspected to confirm complete lysis of the cercariae. For metacercariae, however, the above-mentioned protocol proved ineffective. Therefore, a freeze-thaw cycle was used to weaken the metacercarial cyst wall, followed by DNA extraction using the E.Z.N.A. Tissue Kit. The samples were frozen at −70 °C for 5 min and subsequently incubated at 90 °C for 5 min at 1500 rpm. This cycle was repeated 5 times consecutively. Following thermal treatment, the weakened cyst walls were mechanically disrupted by gently compressing the cyst between a glass slide and a cover slip prior to DNA extraction. For each shedding snail, DNA concentration was quantified using a Qubit™ fluorometer for 2 of the 4 extracted cercariae. All DNA extracts were stored undiluted at −20 °C.

Rapid diagnostic PCR (RD-PCR)

All snail DNA extracts were first screened using a rapid diagnostic PCR (RD-PCR) protocol as described in Carolus et al. (2019). This multiplex assay enables the simultaneous detection of any trematode infection and specific infections by *Fasciola* spp., using a general trematode marker (*18S rDNA*), an internal control marker targeting snails (*18S rDNA*) and a *Fasciola*-specific, high-copy non-coding nuclear repeat (a 124 bp repetitive element) that facilitates sensitive detection of *Fasciola* spp. (Kaplan et al., 1995; Krämer and Schnieder, 1998). PCR reactions were performed in a volume of 15 µL containing 1 µL DNA, 5 µL dH_2O, 1.5 µL primer mix and 7.5 µL Qiagen Multiplex Mastermix. The final mix primer concentrations were 0.2 µM for 18S_Digenea_F and 18S_Digenea_R, 0.1 µM for FW_SNAIL2 and REV_SNAIL2 and 0.6 µM for Kaplan_F and Kaplan_R. Each PCR plate included

https://doi.org/10.1017/S0031182026102728

positive controls consisting of DNA from an adult *F. gigantica* specimen and a mixed DNA sample containing both *P. columella* and *F. gigantica* DNA, as well as a negative control containing nuclease-free water. Amplification products were separated by gel electrophoresis on a 3% agarose gel run at 120 V for 105 min. Bands were visualized using Midori Green Direct staining and UV illumination.

Species identification and DNA barcoding

All adult trematodes and cercariae for which DNA had been extracted and all trematode infections detected through the RD-PCR assay were selected for molecular identification. This was done by sequencing segments of the mitochondrial cytochrome c oxidase subunit I (*COI*) gene and the nuclear ribosomal DNA (*rDNA*) region, including the complete internal transcribed spacer 1 and 2 (*ITS1* and *2*) and the *5.8S rDNA*. For snail species identification, a fragment of the mitochondrial *COI* gene was amplified. A maximum of 2 snails per morphotype per site were selected for sequencing. All primer combinations and PCR protocols followed those described in Schols et al. (2021). Amplifications were carried out using the Qiagen™ *Taq* DNA Polymerase kit in 20 µL reaction volumes, composed of 2 µL DNA extract, 2 µL 10× PCR buffer, 0.6 µL deoxyribonucleoside triphosphate (dNTP) mix (5 mM), 1.2 µL $MgCl_2$ (25 mM), 0.8 µL of each primer (20 µM), 12.68 µL Milli-Q water and 0.12 µL of *Taq* Polymerase. Thermal cycling was conducted on a Biometra™ TProfessional thermocycler and consisted of an initial denaturation at 94 °C for 5 min, followed by 39 cycles of denaturation at 94 °C for 30 s, primer-specific annealing and elongation steps (Schols et al., 2021), and a final elongation step at 72 °C for 10 min. For the parasites, primers used for the *COI* barcoding region were COI1_DIG_F, COI1_DIG_R, COI2_DIG_F, COI2_DIG_R and NASMIT_R (Hammoud et al., 2022; 0.8 µM forward primer and 0.8 µM reverse primer). For amplification of the *ITS* region, we used ITS2_DIG_F and ITS2_DIG_R (Hammoud et al., 2022; 0.8 µM forward primer and 0.8 µM reverse primer), as well as ITS4 and ITS5 (White et al., 1990; 0.8 µM forward primer and 0.8 µM reverse primer). For snails, universal HCO and LCO primers were used (Folmer et al., 1994). All primer sequences and annealing temperatures are listed in Schols et al. (2021). PCR products were visualized on a 1.5% agarose gel stained with Midori Green Direct® and examined under UV light. Samples that showed a clear band were purified using the ExoSAP-IT™ PCR Product Cleanup protocol and sent to Macrogen™ Europe for bidirectional Sanger sequencing using the same primers as those used for amplification.

Phylogenetic analysis

Sequences were processed in Geneious Prime® (v.2025.1.2); chromatograms were visually inspected and ambiguous base calls were resolved or coded using the International Union of Pure and Applied Chemistry (IUPAC) ambiguity codes prior to and following consensus sequence generation. Sequences of the coding marker *COI* were inspected for the absence of stop codons and the correct start codon. All sequences are available on GenBank (see Data Availability Statement). Alignments were made using MAFFT v.7.526 (Katoh et al., 2002). Uncorrected pairwise distances were calculated using MEGA11 (Tamura et al., 2021). Thresholds for species differentiation were p-distance values >5% for *COI* and >1% for *ITS* sequences (Vilas et al., 2005; Lawton et al., 2015). For multiple sequences belonging to the same species, the longest sequence was selected for species identification using the Basic Local Alignment Search Tool (BLAST) on GenBank (Altschul et al., 1990). Since BLAST results did not unambiguously confirm *Calicophoron* species identity, published sequences of all members of *Calicophoron* represented by overlapping *COI* or *ITS2* fragments were downloaded for further phylogenetic analysis along with a representative subset of our samples. The related species *Gigantocotyle gigantocotyle* (Brandes in Otto, 1896) Näsmark, 1937, a member of the same family (Paramphistomidae), was selected as the outgroup for phylogenetic inference because previous analyses place it basally relative to *Calicophoron* (Schols et al., 2025). Sequences of the resulting 16 taxa were first aligned per marker in Aliview v.1.26 (Larsson, 2014) using MAFFT and visually inspected.

Substitution saturation was inspected for each codon position of the rapidly mutating *COI* marker by inspecting the I_{ss} and $I_{ss.c}$ values obtained through Xia's method, which is an information entropy-based index of substitution saturation. In addition, the suitability of the outgroup was assessed through Steel's method, which is based on the parsimony method, in DAMBE v.7.3.37, https://dambe.bio.uottawa.ca/DAMBE/dambe.aspx (Xia, 2018). The outgroup was suitable, and no substitution saturation was detected for codon positions 1 and 2. However, codon position 3 did reveal nonsignificant ($P = 0.43$) substitution saturation ($I_{ss} = 0.6151 > I_{ss.c} = 0.5890$) for a symmetrical tree topology and a significant ($P = 0$) substitution saturation ($I_{ss} = 0.6151 > I_{ss.c} = 0.3588$) for an asymmetrical tree topology. This was taken into consideration during the subsequent analyses by providing a separate substitution model for codon position 3 of the *COI* marker (see below).

The *ITS2* and *COI* alignments were then curated using the least stringent settings in the online web interface of Gblocks (https://ngphylogeny.fr/; Lemoine et al., 2019). Next, a concatenated alignment of both markers (*COI*: 519 sites, *ITS2*: 270 sites) was generated using Mesquite v.3.5 (Maddison and Maddison, 2023). Using the greedy search algorithm and the Bayesian Information Criterion (BIC), the best partition scheme and best-fit substitution models were estimated in PartitionFinder 2 (Guindon et al., 2010; Lanfear et al., 2012, 2017). Partition 1 contained the first and second *COI* codon positions and the *ITS2* sites (688 sites) and was analysed using the Hasegawa–Kishino–Yano substitution model (Hasegawa et al., 1985) with an invariant site correction. Partition 2 contained the third codon position of *COI* (173 sites) and was analysed using the transition (TIM) substitution model with a gamma site correction (Posada, 2003).

Phylogenetic reconstructions were performed using maximum likelihood (ML) and Bayesian inference through the CIPRES Science Gateway v.3.3; https://www.phylo.org/por-tal2 (Miller et al., 2010). ML analyses were conducted in GARLI v.2.10 (Zwickl, 2006). Multiple GARLI runs to determine the best tree converged on the same likelihood (−2,816.12), indicating a stable ML solution. Next, node supports were assessed from 1,000 bootstrap replicates obtained from 20 independent runs of 50 replicates each. Bootstrap values were then summarized on the best ML tree, and nodes with a nodal support value below 50% were collapsed using SumTree v.4.6.1, run in DendroPy v.4.6.1 (Moreno et al., 2024). Bayesian inference was performed using MrBayes v.3.2.7a (Ronquist et al., 2012), with 2 parallel runs containing 4 chains each for 10 million generations. Parameters were estimated independently for each partition [unlink statefreq = (all) revmat = (all) shape = (all) pinvar = (all) tratio = (all)]. Trees were sampled every 100th generation and were used to reconstruct a 50% majority rule consensus tree after discarding the first 25% as *burn-in*. The

https://doi.org/10.1017/S0031182026102728

MrBayes log files were inspected in Tracer v.1.7.1 (Rambaut et al., 2018) to ensure an effective sample size above 200 for all parameters and a caterpillar-like pattern in the trace plot. The resulting trees were rooted using *G. gigantocotyle* as the outgroup in FigTree v.1.4.4. Final adjustments were made in Inkscape v.1.3, including repositioning misplaced support values, adding the bootstrap support values to the Bayesian inference and italicizing species names.

The phylogenetic signal for each separate marker was assessed to confirm that the concatenated analysis is justified. The Gblocks-curated *COI* and *ITS2* alignments were analysed using the ML method in MEGA X (Kumar et al., 2018) with the same best-fit substitution models as the concatenated analysis and with 100 bootstrap replicates. For *COI*, the dataset was analysed with all codons, only codons 1 and 2, and finally with codon 3 only. *COI* codon 3 did not follow the substitution model of the concatenated analysis, as MEGA X does not offer TIM. The General Time-Reversible model (GTR) (Rodríguez et al., 1990) with a gamma correction showed only marginally different BIC and Akaike Information Criterion (AIC) values and was therefore used to analyse this dataset. Sequences spanning less than 75% of the alignment were removed. For *COI*, all 5 sequences from our specimens were retained in the alignment given the substantial genetic variation between them. In contrast, the longest *ITS2* sequence was chosen to represent all our specimens, as they were 100% identical. This resulted in 12 taxa being included for *COI*, spanning 519 bp, and 10 taxa being included for *ITS2*, spanning 315 bp.

Similarly, trematode infections detected in snails with inconclusive BLAST output were integrated with Aliview (MAFFT) into the curated partial *COI* dataset of Schols et al. (2020) to obtain higher-level taxonomic information. The resulting dataset was analysed using the ML method in MEGA X with 1,000 bootstrap replicates and the GTR model with a gamma correction. This resulted in sequences of 27 taxa in an alignment of 306 bp.

Results

Buffalo post-mortem and infecting trematodes

The animal was severely emaciated, with an estimated body mass of 250–300 kg compared to a typical healthy weight of 450–680 kg (Grobler, 1996), prominently protruding hip bones and an almost complete absence of subcutaneous/body fat. The coat was almost completely absent. No ticks were found on the animal. Post-mortem examination revealed extensive accumulation of extracellular fluid within the body cavity, consistent with effusion. The lung showed clear signs of trauma, likely associated with ribcage damage; however, it remains unclear whether this injury occurred ante- or post-mortem, as the carcass had been moved using a vehicle. Urine was clear and odourless. Multiple light-yellow-coloured abscesses or cyst-like structures were observed on the intestinal wall.

No blood flukes were detected in the mesenteric veins, although only a limited section of the vasculature was examined due to time constraints. In the stomach, trematodes were present exclusively in the rumen, where a total of 35 stomach flukes were recovered, rinsed in saline solution and preserved in 70% ethanol. The liver exhibited marked calcification, and dense aggregations of liver flukes were observed within the bile ducts, in some cases appearing to obstruct bile flow. Approximately 50 liver flukes were present in and collected from the liver bile ducts. The initial batch of liver flukes (est. $n = 30$) disintegrated during relaxation in the warm saline solution; therefore, a second batch ($n = 18$) was preserved directly in 70% ethanol without prior relaxation.

Trematode identification

Identification of stomach flukes

Class Trematoda Rudolphi, 1808

Order Plagiorchiida La Rue, 1957

Superfamily Paramphistomoidea Fischoeder, 1901

Family Paramphistomidae Fischoeder, 1901

Genus *Calicophoron* Näsmark, 1937

Calicophoron aff. *microbothrium* (Fischoeder, 1901)

Synonyms and literature of *C. microbothrium*

Paramphistomum microbothrium Fischoeder, 1901; Näsmark (1937), pp 450–452; Eduardo (1983), pp 36–41; Sey (1991), pp 374–377; Chingwena et al. (2002); Pfukenyi and Mukaratirwa (2018); and Sibula et al. (2024b).

Diagnosis of *C. microbothrium*

Diagnosis: length: 3.1–13.0 mm, breadth: 1.4–4.3 mm. Acetabulum subterminal, of the *Paramphistomum* type (*sensu* Näsmark, 1937; Sey, 1991, Fig. 173, p. 86); diameter: 1.28–2.42 mm; number of muscle units, dorsal exterior circular muscle units 1, 10–17; dorsal exterior circular muscle units 2, 23–39; dorsal interior circular muscle units, 29–53; ventral exterior circular muscle units, 10–19; ventral interior circular muscle units, 39–64; and middle exterior circular muscle units, 9–15. Pharynx of the *Calicophoron* type (*sensu* Dinnik, 1964; Sey, 1991, Fig. 58, p. 35); length: 0.38–1.42 mm; and breadth: 0.66–0.93 mm. Terminal genitalium of the *Microbothrium* type (*sensu* Näsmark, 1937; Sey, 1991, Fig. 122, p. 63), located posterior to the oesophageal bifurcation. Pars prostatica almost as long as wide, 0.13–3.67 mm × 0.13–3.46 mm. Large papillae around oral opening extending ventrally to mid-body; small papillae around acetabulum. Excretory pore opening on the dorsal surface at the posterior level of the posterior testis and anterior to the opening of Laurer's canal. Testes tandem, posterior ½ of body: Ant. 0.14–1.79 mm × 0.25–2.76 mm; and Post. 0.62–2.00 mm × 1.14–2.87 mm. Vitellaria lateral; from pharynx to acetabulum; not confluent dorsomedially. Caeca with dorso-ventral bends reach the acetabulum, with blind ends facing dorsally and meeting medially. Mature cercariae are heavily pigmented with 2 eyespots; metacercariae are dome-shaped, measuring 0.14–0.26 mm in diameter (Sey, 1991).

Definitive hosts: *S. caffer* (Sparrman, 1779); *Bos taurus* Linnaeus, 1758; *Bubalus bubalis* Linnaeus, 1758; *Capra nubiana* Cuvier, 1825; *Capra hircus* Linnaeus, 1758; *Damaliscus pygargus* (Pallas, 1767); *Damaliscus korrigum* (Ogilby, 1837); *Gazella gazella* (Pallas, 1766); *Eudorcas thomsonii* (Günther, 1884); *Eudorcas rufifrons* (Gray, 1846); *Hippotragus equinus* (É. Geoffroy Saint-Hilaire, 1803); *Kobus defassa* (Rüppell, 1835); *Kobus kob* (Erxleben, 1777); *Redunca redunca* (Pallas, 1767); *Ourebia ourebi* (Zimmermann, 1783); *Kobus leche* Gray, 1850; *Kobus vardonii* (Livingstone, 1857); *Kobus ellipsiprymnus* (Ogilby, 1833); *Ovis aries* Linnaeus, 1758; *Oryx gazella* (Linnaeus, 1758); *Redunca arundinum* (Boddaert, 1785); *Taurotragus oryx* (Pallas, 1766); *Tragelaphus angasii* Angas, 1849; *Capra ibex* Linnaeus, 1758; and *Camelus dromedarius* Linnaeus, 1758.

Infection site: rumen and reticulum.

Intermediate host: *Bulinus tropicus* (Krauss, 1848); *Bulinus truncatus* (Audouin, 1827); *Bulinus liratus* (Tristram, 1863); *Bulinus forskalii* (Ehrenberg, 1831); *Biomphalaria pfeifferi* (Krauss, 1848); *Bulinus globosus* (Morelet, 1866); and *M. tuberculata* (Müller, 1774).

Type locality: Africa/Sudan. Other localities: Africa: Egypt, Kenya, DRC, Chad, Ethiopia, Angola, Zambia, South Africa,

https://doi.org/10.1017/S0031182026102728

Tanzania, Cameroon, Central Africa, Zimbabwe, Uganda, Senegal, Botswana, Mozambique and Lesotho; Europe: Italy, Portugal and France; and Asia: Iraq, Israel and Iran.

Material examined

ZIMBABWE • 2 adult specimens, median sagittal sectioning; Africa: Zimbabwe: Imire Rhino and Wildlife Conservancy; 2023; Schols & Mudavanhu leg.; host: *S. caffer*; host organ: rumen; GenBank: PZ494265 and PZ494149; and RMCA accession codes: RMCA_VERMES_44928 and RMCA_VERMES_44929.

ZIMBABWE • 10 adult specimens, mounted; Africa: Zimbabwe: Imire Rhino and Wildlife Conservancy; 2023; Schols & Mudavanhu leg.; host: *S. caffer*; host organ: rumen; GenBank: PZ494266–PZ494274, PZ494095–PZ494099 and PZ494152–PZ494154; and RMCA accession codes: RMCA_VERMES_44932–RMCA_VERMES_44941.

ZIMBABWE • 2 adult specimens, SEM; Africa: Zimbabwe: Imire Rhino and Wildlife Conservancy; 2023; Schols & Mudavanhu leg.; host: *S. caffer*; host organ: rumen; GenBank: PZ494275, PZ494276, PZ494100 and PZ494101; and RMCA accession codes: RMCA_VERMES_44942–RMCA_VERMES_44943.

ZIMBABWE • 1 metacercaria; Africa: Zimbabwe: Imire Rhino and Wildlife Conservancy; 2023; Schols & Mudavanhu leg.; intermediate host: *P. columella*; GenBank: PZ494094 and PZ494286; and RMCA accession code: RMCA_VERMES_44931.

Morphological identification

The crossing of the excretory duct and Laurer's canal is in line with members of Paramphistominae (Sey, 1991; key to the subfamily of Paramphistomidae p. 308). The conical body with a medium-sized acetabulum, absent genital sucker, developed pars musculosa and a pharynx of the *Calicophoron* type (*sensu* Dinnik, 1964; i.e. anterior, posterior and lip sphincters absent, inner surface of pharynx not covered in papillae, and exterior and middle circular unit weakly developed) confirm that our specimens belong to *Calicophoron* (Sey, 1991; key to the Paramphistominae p. 342). The vertical position of the testes, absence of a true ventral atrium, a terminal genitalium of the *Clavula/Microbothrium* type (*sensu* Näsmark, 1937; Figure 2), located posterior to oesophageal bifurcation, absent esophageal bulb, tegumental papillae large around the oral opening and extending ventrally to mid-body, and the blind cecal ends directed dorsally and meeting medially are all in line with the identification of our specimens as *C. microbothrium* as examined by SEM, whole mounts and median sagittal sectioning (Figure 2, Supplementary Figure 1; Sey (1991); key to the species of *Calicophoron* p. 387). Furthermore, the diameter of the metacercarial cyst (0.25 mm) falls within the size range for *C. microbothrium* reported by Sey (1991), and is heavily pigmented with eyespots visible (Figure 4A).

Notably, nearly all morphological traits overlap to some extent between *C. microbothrium* and the closely related species *Calicophoron clavula* (Näsmark, 1937), with the sole exception that the caeca meet medially in *C. microbothrium*. Several characters traditionally used to differentiate these species appear ambiguous. The differentiation of the genital atria of the *Clavula* and *Microbothrium* types is considered to be unclear, as the genital sphincter is described as 'enormously developed' for the *Clavula* type in Sey (1991), Fig. 104, p. 57, while drawings do not appear to represent a significantly different size. Furthermore, Eduardo (1983) and Sey (1991) do not describe tegumental papillae on the ventral side of the body for *C. clavula* (Näsmark, 1937), while Soliman et al. (2019) do (with matching *ITS* sequences to *C. microbothrium* from Laidemitt et al. (2016), identical to ours; see below under Genetic results).

However, the dorsal exterior circular muscle unit counts ($n = 10$ in RMCA_VERMES_44929 and 18 in RMCA_VERMES_44928) fall outside the known range of *C. microbothrium* (23–39), the mostly obliquely tandem position of the testes, the ridges around the terminal genitalium as examined by SEM (Figure 2C) and the level of the excretory pore posterior to the posterior testes in specimen RMCA_VERMES_44928 do not match the known description of *C. microbothrium* (although this could be due to the noticeably small testes size in this specimen). These differences, yet for the rest, the closest resemblance to *C. microbothrium*, warrant the tentative identification as *C.* aff. *microbothrium*.

Genetic insights on *C.* aff. *microbothrium*

The partial *COI* region was successfully amplified for 5 *C.* aff. *microbothrium* specimens with both primers (GenBank: PZ494149 and PZ494151–54), and for the remaining 10 specimens with a single primer (NASMIT_R, GenBank: PZ494094–PZ494103). Overall, the quality of the sequences generated by the forward primer COI_DIG_F was poor. However, the quality of all non-consensus sequences except one was sufficiently high to be included in the analysis. The resulting sequence lengths varied between 695 and 850 bp, with 0–39 differences between each of the specimens, corresponding to pairwise distances of 0.0–5.2%. The *ITS1-5.8S-ITS2* region of 14 out of 15 specimens was successfully sequenced using the ITS4 primer (GenBank: PZ494265–PZ494278). The strands generated by the ITS5 primer were of poorer quality and were excluded from the analysis. The resulting 14 sequences were 100% identical across the overlapping 891 bp.

For *COI* sequences, all specimens showed the most similar BLAST hits with 2 *Calicophoron* sp. from Zimbabwe (GenBank: PP556552 and MT994280, query coverage 88–90%, host: *B. truncatus* and *B. taurus*) with identity scores ranging from 94.8% (RMCA_VERMES_44942 and GenBank: MT994280) to 99.2% (RMCA_VERMES_44945 and GenBank: MT994280). All other GenBank records showed a low overlap (query coverage <50%) or low similarity (identity scores < 90.6%), with the closest match being *C. clavula* (GenBank: KX670139, query coverage 68–72%, country: Kenya) with identity scores ranging from 90.2% to 90.5%.

For the *ITS1-5.8S-ITS2* region, the most similar BLAST hits were with *Paramphistomum* sp., *Nilocotyle praesphinctris, Calicophoron raja* and *Paramphistomum leydeni* (resp., GenBank: OQ459353, LC660653, LC633276 and PP754894; query coverage 49–52%; all members of Paramphistomidae; hosts: *Canis lupus familiaris, Hippopotamus amphibius, Connochaetes gnou* and *B. taurus*) with identity scores of 99.3%. Notably, only *C. raja, Calicophoron microbothrioides* and *Calicophoron daubneyi* were included as members of *Calicophoron* in the 100 best BLAST results. Pairwise alignment with *C. clavula* and *C. microbothrium* (resp., GenBank: MK416145 and KP639632) revealed 1–4 and 4 mismatches, respectively. However, 1 mismatch in *C. clavula* and 4 in *C. microbothrium* occur at the first nucleotide positions of the GenBank sequences and also mismatch with all other paramphistomid sequences available on GenBank, suggesting they could be erroneous. Excluding these nucleotides reveals a 100% similarity between *C. microbothrium* and all our specimens, and 0–3 mismatches between our specimens and *C. clavula*.

Phylogenetic inference using the ML method did not reveal drastically different tree topologies between the separate marker datasets, justifying the concatenated analysis (Supplementary Figures 2–5). Furthermore, most nodes were

https://doi.org/10.1017/S0031182026102728

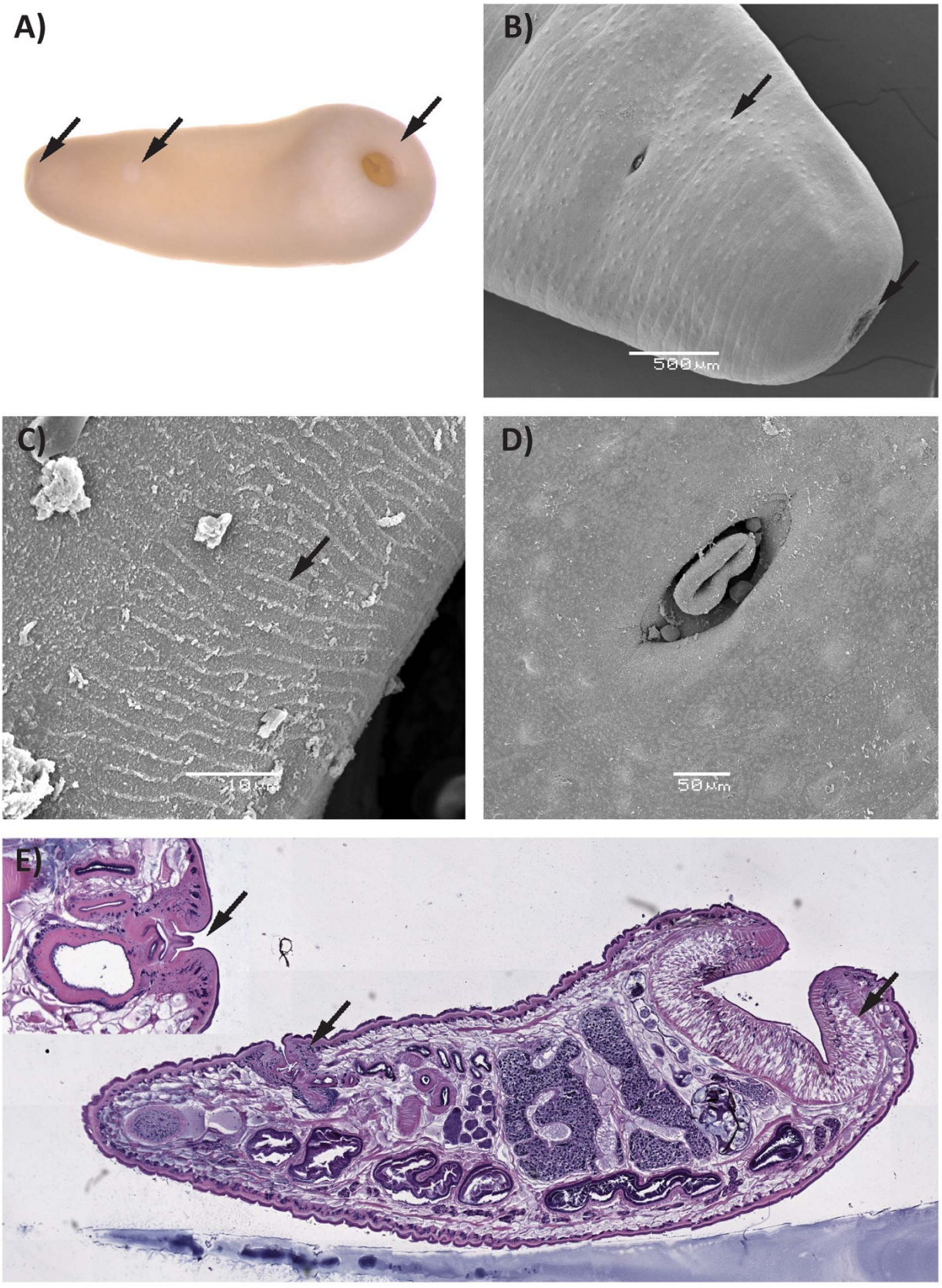

Figure 2. Imaging (A), SEM (B–D) and median sagittal sectioning (E) to visualize different diagnostic traits of *C.* aff. *microbothrium*. (A) Overview of the whole worm, fixed in 70% ethanol. The anterior oral opening is indicated by the left arrow, the terminal genitalium by the middle arrow and the acetabulum by the right arrow. (B) The location and extent of the tegumental papillae (left arrow) in RMCA_VERMES_44942: large around the oral opening (right arrow) and extending ventrally to mid-body. (C) The fine ridges visible near the terminal genitalium of RMCA_VERMES_44942, indicated by an arrow. (D) The frontal view of the terminal genitalium of RMCA_VERMES_44943. (E) Overview of the general morphology of RMCA_VERMES_44929, with the terminal genitalium of RMCA_VERMES_44928 presented as an inset and both terminal genitalia indicated by the left arrows. The right arrow indicates the acetabulum.

https://doi.org/10.1017/S0031182026102728

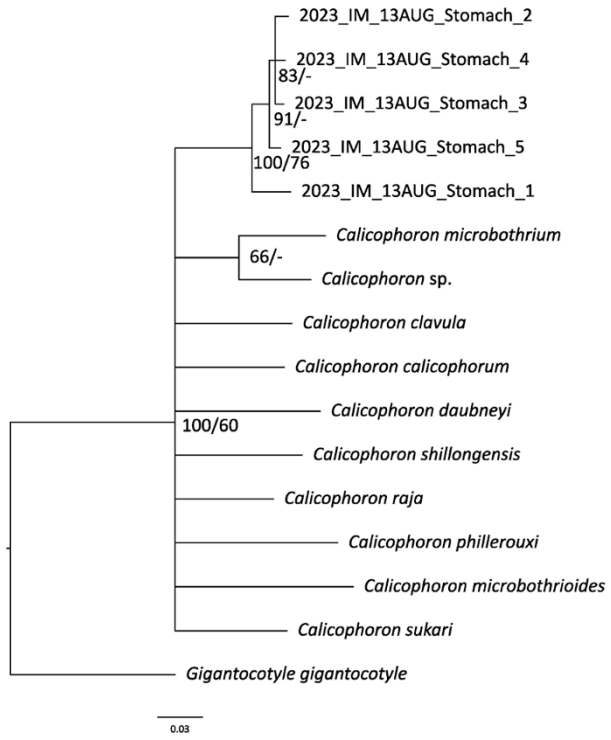

Figure 3. Bayesian phylogenetic inference based on the concatenated *COI* (519 bp) and *ITS2* (341 bp) sequences of *Calicophoron* (860 bp). *Gigantocotyle gigantocotyle* from Paramphistomidae was used as an outgroup to root the tree. Nodal support is indicated as posterior probabilities and bootstrap percentages, respectively, before and after the '/' separator. Nodes with nodal support values below 50 were collapsed. The scale bar indicates 0.03 substitutions per site.

characterized by low nodal support values. This remained in the concatenated analysis (Figure 3), whereby most internal relationships within *Calicophoron* remained weakly supported and collapsed in the majority-rule consensus tree (posterior probability < 50%). Nevertheless, the sequences from *C.* aff. *microbothrium* generated in this study formed a clade separate from available sequences on GenBank.

Identification of liver flukes

The liver flukes were morphologically identified as *F. gigantica* (Figure 4E). *COI* sequencing was successful for 17 out of 18 liver fluke samples (GenBank: PZ494155–PZ494170 and PZ494104), with pairwise distances between the obtained sequences ranging between 0% and 3% for *COI* (>683 bp), while *ITS1-5.8S-ITS2* sequencing was successful for all samples (GenBank: PZ494287–PZ494304), and the resulting sequences were 100% identical (911 bp), confirming that all liver fluke samples belong to the same species (Ai et al., 2011). The selected representative *COI* sequence was 100% identical to 2 *F. gigantica* sequences from cattle in Zimbabwe (GenBank: MT994269 and MK330627). The representative *ITS1-5.8S-ITS2* sequence was 100% identical to several *F. gigantica* sequences from across Africa, including Chad, Kenya and Côte d'Ivoire. BLAST results for both *COI* and *ITS1-5.8S-ITS2* support the identification as *F. gigantica* and do not indicate hybridization.

Snail identification

A total of 728 snails were collected and morphologically identified as the following species: *R. natalensis, P. acuta, P. columella* and a *Lentorbis*-like planorbid (Figure 4). *COI* sequencing was successful for all snails, and morphological identification of *P. acuta, R. natalensis* and *P. columella* was well supported by the BLAST results, with BLAST identities >99% and query coverage >98%. One planorbid remains with an uncertain identification. Morphologically, the *Lentorbis*-like planorbid closely resembles the description of *Lentorbis junodi* (Connolly, 1922): shell height <2 mm, lentiform shell, the absence of internal septa and glossy reddish-brown shell colour (DBL-WHO, 1977, 1986; Brown and Kristensen, 1989). Genetically, all 10 specimens have 100% identical *COI* sequences across 562 bp (GenBank: PZ494122–PZ494131). The closest BLAST match was with Planorbidae sp. (GenBank: LC491289, country: Kenya) with 96.9% identity and 100% query coverage. The second-closest BLAST match was with *Polypylis* sp. (GenBank: LC429542, country: Japan, Planorbidae) with 96% identity and 100% query coverage. It should be noted that no *COI* sequences belonging to representatives of *Lentorbis* and the morphologically similar *Segmentorbis* are currently available on GenBank. However, we received access to unpublished sequences of a *Segmentorbis* sp. (pers. comm. Christian Albrecht) and a tentatively identified *Lentorbis* sp. (pers. comm. Fiona Allan), allowing direct comparison of *COI* sequences across 554 bp. Pairwise distances with *Segmentorbis* sp. were 3.3–4.1% (29683–29684, Christian Albrecht, country: Uganda), and 15.4% with the tentatively identified *Lentorbis* sp. (CQJ265_17772656 and CQJ268_17772687, Fiona Allan, country: Angola).

Trematode diversity in snails and linking life cycles

Six out of the 728 (0.8%) collected snails shed cercariae, while RD-PCR revealed that 76 out of 338 (22.5%) contained trematode DNA. Table 1 shows snail abundance and infection prevalence per snail species per site. Out of the 76 detected infections through RD-PCR, only 9 yielded good-quality sequences for the *COI* marker, of which 6 also yielded good-quality *ITS1-5.8S-ITS2* sequences. None of the collected snails was found infected with *F. gigantica*. In contrast, 1 *P. columella* was infected with *C.* aff. *microbothrium*. This was confirmed by the *COI* sequence of the metacercaria obtained from this snail (GenBank: PZ494094), which was between 94.9% and 98.9% identical to the sequences of the adult stomach flukes. These distances are in line with the 1.6–5.2% pairwise distance seen in the 5 adult *C.* aff. *microbothrium*. The *ITS1-5.8S-ITS2* sequence (GenBank: PZ494286) was 100% identical to the sequences of the adults infecting the buffalo. Furthermore, the top *COI* BLAST hit was the same *Calicophoron* sp. sequence as the adults (99.1% identical, GenBank: MT994280, larval specimen from Zimbabwe), and the top BLAST hits for *ITS2* were *Calicophoron* sp. sequences from Uganda (100% identical, 98% query coverage, GenBank: OQ548160– OQ548168) and *C. microbothrium* from Egypt and Southern Africa (100% identical, 77–80% query coverage, GenBank: OK216192 and KP639635, adults).

One *R. natalensis* individual was shedding xiphidiocercariae that were genetically similar to a prepatent infection in a second *R. natalensis* individual (*COI*: 99.4% identical, GenBank: PZ494148 and PZ494115; *ITS1-5.8S-ITS2*: 100% identical, GenBank:

https://doi.org/10.1017/S0031182026102728

Table 1. Overview of the number of snails per species per site. Columns show the total number of snails that were sampled and how many of those were tested, the number of snails shedding cercariae, and the number of snails that were infected as detected by RD-PCR

	P. acuta			*P. columella*			*R. natalensis*			*Lentorbis*-like planorbid		
Site	Sampled (tested)	Shedding	Infected	Sampled(tested)	Shedding	Infected	Sampled(tested)	Shedding	Infected	Sampled(tested)	Shedding	Infected
G	59 (50)	0	9	13 (13)	0	11[d]	0	0	0	0	0	0
				39 (39)*	2*,[a]	4*						
H	10 (10)	0	0	7 (7)	0	2	1 (1)	0	0	0	0	0
W	431 (50)	0	2	0	0	0	149 (149)	2[b,c]	42[b,c,e]	0	0	0
Q	4 (4)	0	1	0	0	0	5 (5)	0	2	10 (10)	2[f]	3

[a]*C.* aff. *microbothrium* (1 patent infection genetically confirmed, 1 patent infection not genetically confirmed).
[b]*P. maculosus* (1 patent and 1 prepatent infection genetically confirmed).
[c]*Plagiorchis* sp. (1 patent and 2 prepatent infections genetically confirmed).
[d]*Echinostoma* sp. (1 prepatent infection genetically confirmed).
[e]*Echinostoma* sp. (2 prepatent infections genetically confirmed).
[f]A member of Plagiorchiida (2 patent infections genetically confirmed).
*Were sampled outside of the standardized sampling time frame.

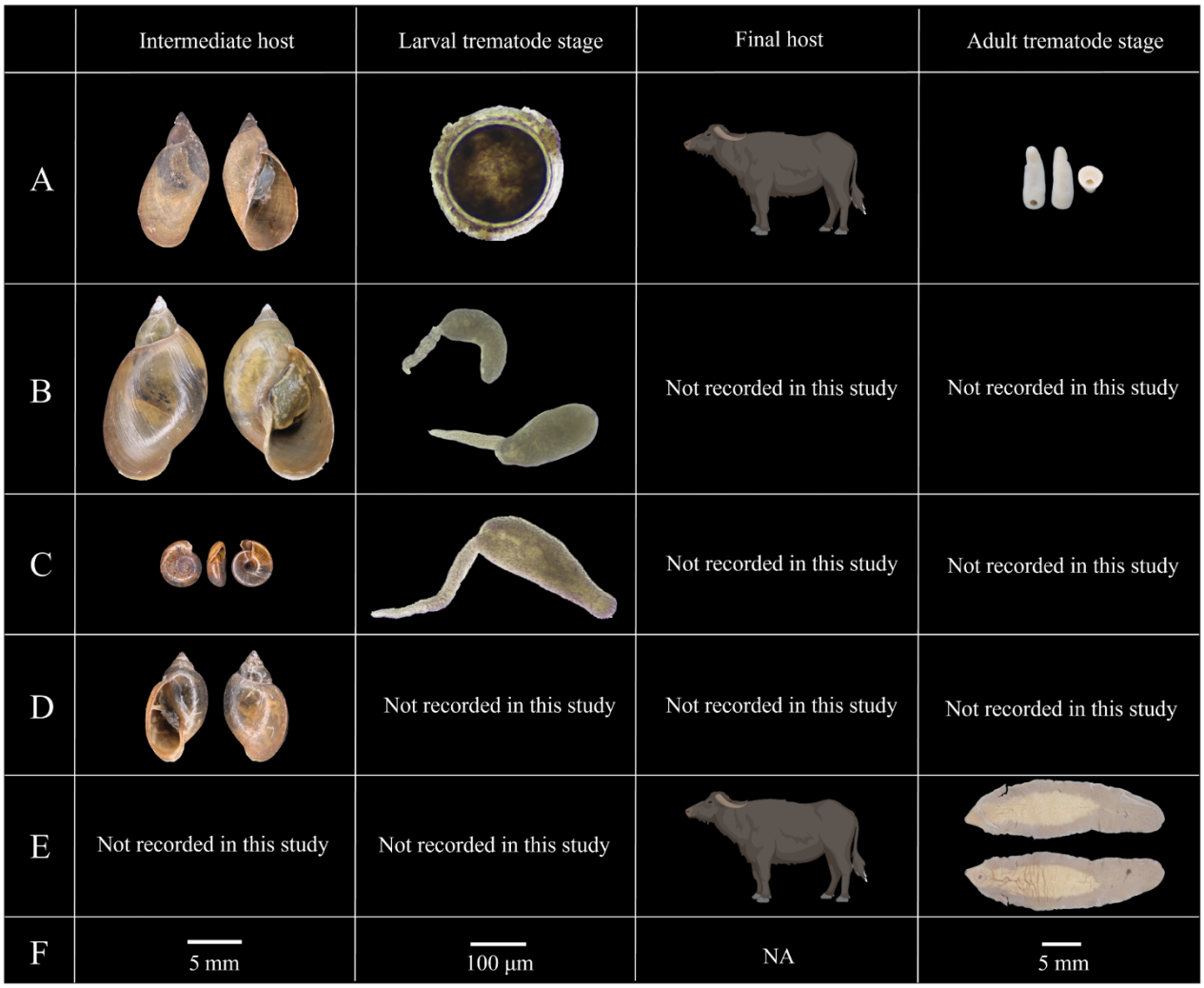

Figure 4. Overview image showing the different freshwater snail species linked to the larval trematode stages, final hosts and adult trematode stages found within the Buffalo-containing section of Imire. (A) *P. columella* was found shedding *C.* aff. *microbothrium*, of which adults were collected from the buffalo. The picture shows a metacercaria that encysted after shedding. (B) *R. natalensis* was found shedding *P. maculosus* (top) and *Plagiorchis* sp. (bottom) cercariae. (C) A *Lentorbis*-like planorbid was found to shed cercariae of a member of the order Plagiorchiida. (D) *P. acuta* did not release any cercariae. (E) *F. gigantica* was only found in the adult stage within the buffalo and could not be linked to active infections in any of the collected snails. (F) Scale bar. Molecular screening additionally revealed that both *P. columella* and *R. natalensis* were also infected with an *Echinostoma* sp. (non-shedding infections).

PZ494284, PZ494279 and PZ494280). Both infections were identified with caution as *Plagiorchis maculosus* based on BLAST results (*COI*: >99.2% identical and 100% query coverage, GenBank: NC_042482, adult; and *ITS1-5.8S-ITS2*: >99.6% identical and 100% query coverage, GenBank: PV650291, life stage unknown). Another *R. natalensis* individual was also shedding xiphidiocercariae that were genetically identical to infections in 2 other non-shedding individuals for both the *COI* and *ITS1-5.8S-ITS2* sequences (GenBank: PZ494150, PZ494116, PZ494117, PZ494281 and PZ494285). This trematode was identified as *Plagiorchis* sp. given that the longest cercarial *ITS* sequence (1097 bp) was 100% identical to an adult *Plagiorchis* sp. sequence from mice in Senegal (Catalano et al., 2019), and the second-best hits all belonged to *Plagiorchis* sp. as well. The BLAST results for *COI* also pointed towards *Plagiorchis*, with top hits all being *Plagiorchis* sp. and between 87.3% and 97.9% identical to our sequence. Cercariae of both *Plagiorchis* spp. were xiphidiocercariae and shared the following characteristics: a clear stylet and a simple tail without finfolds, shorter than the body (Figure 4B). A third trematode infecting 2 *R. natalensis* and 1 *P. columella* snail was only revealed through RD-PCR, as the 3 infected snails did not shed any cercariae (GenBank: PZ494118, PZ494092, PZ494093 and PZ494282). The resulting *COI* sequences revealed that the trematodes causing these 3 infections belong to the same species (176 bp, *COI*: 99.4–100%, *ITS1-5.8S-ITS2* sequencing was only successful for 1 out of 3 infections). The longest *COI* fragment (413 bp from *P. columella*) showed the closest affinity to the *Echinostoma revolutum* complex (91–98.6% identical, adults), and the *ITS1-5.8S-ITS2* sequence from the same *P. columella* snail showed close affinity to *E. revolutum* as well (97.6–99.1% identical, adults). However, this is a species complex comprising more than 57 species, and only *E. caproni* and *E. deserticum* have been reported from the African continent (Chai et al., 2020). Therefore, this trematode is identified as *Echinostoma* sp.

The cercariae and infections isolated from the *Lentorbis*-like planorbid were successfully sequenced and are curated in the

https://doi.org/10.1017/S0031182026102728

RMCA collection (GenBank: PZ494147 and PZ494283; RMCA codes: 3 cercariae as RMCA_VERMES_44925 parasites of BE_RMCA_MOL.Gas.923936 and 1 cercaria as RMCA_VERMES_44926 parasites of BE_RMCA_MOL.Gas.923939). All sequenced cercariae and infections were 100% identical across specimens and markers (*COI* and *ITS1-5.8S-ITS2*). However, the sequences yielded no significant BLAST matches, with the closest match for *COI* being *Paragonimus mexicanus* (82.1% identical). The *ITS1-5.8S-ITS2* sequences were 98.7% identical to *Lepocreadium trulla* (GenBank: KU527433, host: marine ray-finned fish *Lutjanus campechanus*, country: USA, order: Plagiorchiida), although query coverage was only 41%. The closest match with 100% coverage was *Ribeiroia* sp. (88.9% identical, GenBank: OQ549868, host: freshwater snail *B. tropicus*, country: Uganda, order: Plagiorchiida). Phylogenetic inference further supports the classification of this parasite as a member of the order Plagiorchiida (Supplementary Figure 6). The cercariae were xiphidiocercariae (Figure 4C) with a clear stylet, a tail without finfolds and the ventral sucker smaller than the oral sucker (28.8 and 45.7 µm, respectively). The total body length was 287 µm, almost equal to the tail length (290 µm).

Discussion

This work integrates wildlife parasitology, molecular approaches and classical snail surveys to elucidate trematode epidemiology across life stages within a managed wildlife conservancy. Moreover, the co-occurrence of multiple trematode taxa within shared snail and vertebrate hosts is increasingly recognized as a key modulator of infection intensity, transmission success and disease outcome (Sousa, 2015; Laidemitt et al., 2019). Therefore, a comprehensive understanding of the entire snail and trematode community within a system is imperative for identifying the drivers behind infection outcome.

Two trematode species were found infecting the weakened buffalo: *F. gigantica* and *C.* aff. *microbothrium*. The integrative taxonomic approach in this study resulted in the designation of the stomach flukes as *C.* aff. *microbothrium*, but also highlighted inconsistencies in certain diagnostic morphological traits within *Calicophoron*, such as the genital atria and tegumental papillae. As expected, the applied molecular markers showed contrasting patterns from a species identification perspective. The *ITS* region displayed very limited variation both within species (all sequences identical) and between species (pairwise distance 0.3–2.5%), supporting its usefulness as a conservative marker for confirming species identity (Laidemitt et al., 2016). In contrast, *COI* exhibited substantially higher divergence between species (8.3–15%) and notable intraspecific variation (up to 5.2%). This higher variability is consistent with the rapid accumulation of genetic variation reported for *COI* in amphistomes (Laidemitt et al., 2016) and other animal groups (Mueller, 2006). While such variability can complicate the establishment of clear genetic thresholds, it also provides discriminatory power at the species and population level. The concatenated analysis recovered *C.* aff. *microbothrium* as a single clade, clearly separated from previously generated *C. clavula* and *C. microbothrium* sequences. Although clustering of specimens from the same locality is not unexpected, the combined *COI* and *ITS* dataset supports their consistent assignment to a single taxonomic entity. Given the persistent uncertainty surrounding species boundaries in *Calicophoron* and other amphistomes (Laidemitt et al., 2016; Schols et al., 2025), the continued use of *COI* and *ITS* in a barcoding framework remains valuable, provided that thresholds are applied cautiously and within an integrative taxonomic context including morphological and ecological data. When the same dataset is considered from a phylogenetic perspective, however, its limitations become apparent. Most internal relationships within *Calicophoron* remained weakly supported and collapsed in the concatenated majority-rule consensus tree (posterior probability $< 50\%$), indicating a lack of phylogenetic signal for resolving deeper relationships among species. Completely abandoning standard DNA barcoding regions is not necessarily warranted, but expanding marker choice, including, for example, *28S rDNA*, would likely improve phylogenetic resolution and contribute to more robust reference databases (Blasco-Costa et al., 2016).

Calicophoron microbothrium, possibly a species complex (Laidemitt et al., 2019), is the most widespread amphistome species in Africa and has been reported to infect 24 other African wild ruminant species besides African buffalo, as well as cattle, goats and sheep (Sey, 1991; Sibula et al., 2024b). Despite their widespread and increasing prevalence in domestic ruminants, the economic impact of amphistome infections remains poorly understood and is likely underestimated in Eastern and Southern Africa, underscoring the need for further research in the region (Pfukenyi and Mukaratirwa, 2018). To our knowledge, we provide the first report of a natural and patent infection of a member of *Calicophoron, C.* aff. *microbothrium*, in the invasive exotic North American snail *P. columella* and with extension to any member of Lymnaeidae (Dinnik, 1962; Chingwena et al., 2002). So far, only *C. daubneyi* (Dinnik, 1962) has been shown to experimentally infect *P. columella*, although infection was only sustained in immature snails in a laboratory environment (Dar et al., 2015). This finding could have great implications for the transmission of *C.* aff. *microbothrium* and consequently impact the health of domestic and wild ruminant populations across the invasive range of *P. columella* (countries and territories with confirmed records of *P. columella*: Egypt, Eswatini, Kenya, La Réunion, Malawi, Mayotte, Namibia, South Africa, Zambia and Zimbabwe; Jones et al., 2024; Schols and Huyse, 2024). It highlights the potential for a similar scenario to that documented for *P. columella* and *Fasciola* spp. in Africa, where the invasive snail acts as a highly susceptible intermediate host, driving parasite spillback and boosting transmission to local final hosts, with implications for both cattle and wildlife health (Grabner et al., 2014; Malatji and Mukaratirwa, 2020; Schols et al., 2021; Outa et al., 2024). The absence of prior *Calicophoron* records in *P. columella* likely reflects historical detection bias, as molecular xenomonitoring for amphistomes in freshwater snails across Africa has only recently gained traction (Sibula et al., 2024a). Furthermore, established paradigms prioritizing intermediate host species of *Bulinus, Biomphalaria* and *Galba* (Laidemitt et al., 2016; Sibula et al., 2024b), reliance on conventional visual shedding assays and the rapid encystment of *Calicophoron* cercariae have likely caused this association to be systematically overlooked.

In Imire, no *Fasciola* spp. infections have been reported in *P. columella* so far, despite its reported role in *Fasciola* transmission and the numerous fasciolosis cases within the conservancy (this study; Mudavanhu et al., 2024a; pers. comm. Karl van Laeren and autopsy report Jacqueline De Grant). Notably, *Fasciola* infections were also absent in snails sampled in August 2021 (Mudavanhu et al., 2024b), while Mudavanhu et al. (2024a) identified a single *F. gigantica* infection in *R. natalensis* in the middle section at Imire in the warm, wet season of 2022. *Fasciola* prevalence in snails is generally low compared to the high infection prevalence in the final hosts, although this is the case for all trematode species (Pfukenyi

https://doi.org/10.1017/S0031182026102728

et al., 2006; Hadebe et al., 2023). Moreover, seasonal variation is a typical phenomenon, with *Fasciola* egg hatching and development being optimal between 20 °C and 30 °C (stopping below 10 °C), while miracidia hatching and cercarial development times increase significantly with decreasing temperature (Modabbernia et al., 2024). As such, the cold, dry season in which sampling took place could be suboptimal for *F. gigantica* development, which possibly explains the absence of infected snails. However, in samples collected during the same period from the central section of the conservancy, multiple specimens of both *R. natalensis* and *P. columella* were found infected with *Fasciola* spp. using the same RD-PCR protocol (unpublished results). This suggests that seasonality alone is unlikely to account for the absence of infected snails in the present study. Furthermore, host–parasite incompatibility is unlikely, as invasive African *P. columella* populations belong to a globally distributed, highly susceptible clone (Lounnas et al., 2017). Instead, this discrepancy underscores the focal nature of *Fasciola* transmission and low prevalence in snail intermediate hosts. Field screenings frequently fail to detect infected snails even in active foci, a pattern well documented in endemic settings where screening hundreds of lymnaeid snails by PCR returned zero infections despite >50% prevalence in local livestock (Hoang Quang et al., 2026).

Another consideration is the yearly treatment of the conservancy's ruminants with the anthelmintic Flukazole C, a highly effective drug against liver flukes if dosed correctly (Hutchinson et al., 2009), which could affect the number of eggs that are released and subsequently infect snails (Kouadio et al., 2021). In this case, however, administration is done annually through supplemental feeding, which makes accurate dosing nearly impossible for free-roaming animals. Furthermore, no literature describing the efficacy of this drug against amphistomes was found, and other flukicides tend to show only limited efficacy against amphistomes, especially against immature stages (Huson et al., 2017). Therefore, *F. gigantica* and *C.* aff. *microbothrium* will likely be able to persist and co-infect local ruminants in the coming years unless treatment methods change.

Shedding experiments and RD-PCR confirmed the presence of additional trematodes. As expected, RD-PCR revealed more trematode infections than shedding (Born-Torrijos et al., 2014). However, many of the amplification and sequencing attempts for the molecularly detected infections failed. This is probably due to the limited set of available *COI* primers for African trematodes, combined with low trematode DNA template within snail tissue. Therefore, isolating trematode parthenitae from dissected snails might be beneficial in future studies. *Radix natalensis* was infected with *P. maculosus* and an unidentified *Plagiorchis* species. Trematodes of this genus are widely distributed and infect freshwater snails as first intermediate hosts, insect larvae as second intermediate hosts and a diverse range of final hosts, including birds and mammals, and some species are zoonotic (Chai, 2019). Knowledge of *Plagiorchis* spp. in Africa is scarce; however, *P. maculosus* has been reported once from *Hirundo rustica* in Togo (Chai, 2019). Given that only a single top BLAST match corresponds to a morphologically verified adult specimen, this identification should be interpreted with caution. Our *Plagiorchis* sp. sequences were identical to those of a previously undescribed *Plagiorchis* species in *R. natalensis* and mice from Senegal, reported by Catalano et al. (2019).

Echinostoma sp. was found infecting *R. natalensis* and *P. columella*. Echinostomatids typically infect freshwater snails as a first intermediate host; a broad range of aquatic organisms as second intermediate hosts, including but not limited to snails, frogs, clams and fish; and birds and mammals as definitive hosts (Toledo and Fried, 2019). The host snails reported here are consistent with those reported in the literature (Grabner et al., 2014; Chibwana and Nkwengulila, 2019).

Finally, the *Lentorbis*-like planorbid was found infected with a species of the order Plagiorchiida, which could not be further identified. Morphologically, the *Lentorbis*-like planorbid closely resembles the description of *L. junodi*, which is known to occur, albeit rarely, from Ethiopia to South Africa, matching its occurrence in Zimbabwe (DBL-WHO, 1977, 1986; Brown and Kristensen, 1989). The pairwise distance of 3.3–4.1% with *Segmentorbis* sp. is close to the intergeneric threshold of 4–6% frequently seen for Planorbidae (pers. comm. Christian Albrecht). Combined with the absence of internal septa, the genetic distance indicates that the *Lentorbis*-like planorbid belongs to a genus closely related to *Segmentorbis*, which could potentially be *Lentorbis*. Combined, this suggests that our specimen could be identified as *Lentorbis* cf. *junodi*. However, the pairwise distance of 15.4% with the tentatively identified *Lentorbis* sp. (Angola) suggests that one of the specimens is wrongly identified as *Lentorbis*. Soft tissue morphology, together with comparison to type material, should provide a definite species identification (Brown and Kristensen, 1989). Therefore, the classification of our specimens remains as *Lentorbis*-like planorbid. Clearly, African small planorbids and their parasites remain largely unexplored, and this underrepresentation has also been reported in Europe (Schwelm et al., 2018). A taxonomic effort is required to fully map their diversity across Africa. In turn, this will facilitate future barcoding efforts and provide the basis for a more profound understanding of snail host–parasite interactions across Africa (Brooks, 1988; Kamiya et al., 2014; Engelstädter and Fortuna, 2019).

Although buffalo mortality is typically higher during winter months due to limited resources and low temperatures (Prins et al., 2023; Taylor et al., 2023), the number of fatalities observed in the winter of 2023 (26 wild ruminants, including 4 juvenile buffaloes) was substantially higher than in previous years. This increase occurred despite reportedly milder conditions, with frost starting approximately 1 month later than usual and the provision of supplemental feeding. The presented data do not directly confirm trematode infections as the main cause of this individual buffalo's condition, either. These observations suggest that additional factors may have contributed to the observed increase in mortality. Malnutrition and stress reduce buffaloes' resilience to disease, and increased parasite and pathogen transmission is more likely to occur during droughts when animals aggregate around water sources (Kock et al., 2023). In addition, trematode infections have been linked to an increased susceptibility to pathogens and more severe disease in buffaloes and cattle (Abruzzi and Fried, 2011; Ezenwa and Jolles, 2011; Howell et al., 2018). For instance, buffaloes with bovine tuberculosis that were also infected with helminths suffered higher mortality compared to those treated with anthelmintics (Ezenwa and Jolles, 2015). Environmental stress is known to affect parasite burden in other vertebrates as well (Oppliger et al., 1998; Lafferty and Kuris, 1999; Vicente-Santos et al., 2023). For instance, pesticide exposure suppresses immune responses in frogs, leading to increased trematode infections (Kiesecker, 2002). Therefore, we propose that trematode infections in large African herbivores may act as an additional stressor, most pronounced under conditions of environmental stress and exacerbated by anthropogenic pressures and co-infections with other pathogens. A multiple-stressor approach is required to test this hypothesis, in which individual-level samples are collected to

https://doi.org/10.1017/S0031182026102728

measure physiological and immunological phenotypes in order to determine patterns of wildlife health across stressful time periods and landscapes (Pirotta et al., 2022; Simonis et al., 2025). Nevertheless, it will be a challenging effort; solutions such as non-invasive (stool or blood) sampling are needed to facilitate ethical parasite sampling in living mammals, complex interactions need to be considered and confounding snail and parasite identification needs to be overcome.

In conclusion, this study highlights the complex interactions between trematodes, invasive snail species and wildlife health in an intensively managed wildlife conservancy. We reported *F. gigantica* and *C.* aff. *microbothrium* in a deceased African buffalo and provide novel evidence that the invasive snail *P. columella* can naturally sustain and transmit *C.* aff. *microbothrium*, a major cause of amphistomiasis of African ruminants. This finding further highlights the potential role of this invasive snail in parasite spillback and elevated trematode transmission. Based on these results, we suggest that the role of trematodes as additional stressors should not be underestimated when environmental stress is high or potential pathogen co-infections occur. Finally, this study encountered persistent taxonomic and knowledge gaps in African trematodes and freshwater snails, emphasizing the need for frequent monitoring using an integrated molecular, morphological and ecological approach to better understand parasite diversity, transmission dynamics and their implications for wildlife health in rapidly changing ecosystems.

Supplementary material. The supplementary material for this article can be found at https://doi.org/10.1017/S0031182026102728.

Data availability statement. DNA and specimen vouchers of all studied parasites and snails are stored in the RMCA's collection (RMCA_VERMES_44925–RMCA_VERMES_44964, BE_RMCA_MOL.Gas.923936–BE_RMCA_MOL.Gas.923939 and BE_RMCA_MOL.Gas.923949–BE_RMCA_MOL.Gas.924205) and are available with a completed Materials Transfer Agreement. All sequences generated in this study are available on the public repository NCBI GenBank under the accession numbers PZ494092–PZ494104, PZ494115–PZ494170, PZ494279–PZ494304 and PZ494265–PZ494278.

Acknowledgements. The authors want to thank Reilly Travers, the manager of Imire, for facilitating the sampling effort within the reserve. They also acknowledge Kalle Lambaerts' assistance with the molecular work, Rudy Jocqué for his help with SEM imaging, Natascha Steffanie for preparing the stomach fluke sections and Arnaud Henrard for curating the samples in the RMCA collection. Noortje Verbruggen is thanked for her help with sampling, and Karl Van Laeren and Jacqueline De Grant are thanked for their veterinary perspectives and input. Fiona Allen, Christian Albrecht and Maxim Vinarski are thanked for their time and assistance in identifying the *Lentorbis*-like planorbid specimens, and Martina Laidemitt for her perspective on the *C.* aff. *microbothrium* identification and additional imaging efforts.

Author contributions. Conceptualization: E.G., R.S., A.M. and T.H.; data collection: R.S., A.M. and T.M.; formal analysis: E.G. and R.S.; investigation: E.G. and R.S.; resources: T.M. and T.H.; funding acquisition: E.G., R.S., A.M., T.M., J.M., M.V. and T.H.; data curation: E.G. and R.S.; writing – original draft: E.G. and R.S.; writing – review and editing: E.G., R.S., A.M., T.M., J.M., M.V. and T.H.; and supervision: M.V. and T.H. All authors read and approved the final manuscript. E.G. and R.S. contributed equally.

Financial support. Fieldwork was supported by the Research Foundation-Flanders (FWO-Vlaanderen) as a grant for a short study visit abroad (K225223N). R.S. was supported by BRAIN-be 2.0 under the MicroResist project (B2/191/P1/ MicroResist) and through the KU Leuven (Grant No. PDMT2/24/045). E.G. was partly supported through the MicroResist Project and partly by the FWO PhD fellowship in fundamental research (11A0D25N) and the Special Research Fund (BOF) of Hasselt University BOF24INCENT23. Part of the infrastructure used was supported by EMBRC Belgium, FWO project GOH3817N. A.M. was supported by VLIRUOS through its Global Minds PhD fellowship 3E210232.

Competing interests. The authors declare that there are no conflicts of interest.

Ethical standards. Ethical permission to conduct the study in Zimbabwe was obtained through the National Animal Research Ethics Committee (NAREC, Contract No: 006/2020). This approval covered the collection of freshwater snails and their associated trematode larval stages, as well as the recovery of adult flukes from abattoirs and from vertebrates that were culled or found dead within wildlife conservancies. The Biosafety Export permit was obtained through the National Biotechnology Authority (permit code: BEP0009234). The import permit to Belgium was authorized by the Federal Agency for the Safety of the Food Chain (Federaal Agentschap voor de Veiligheid van de Voedselketen, FAVV; permit code: 2023DBP258).

References

Abruzzi A and Fried B (2011) Coinfection of *Schistosoma* (Trematoda) with Bacteria, Protozoa and Helminths. In Rollinson D and Hay SI (eds.), *Advances in Parasitology*. London: Academic Press, 1–85.

Ai L, Chen M-X, Alasaad S, Elsheikha HM, Li J, Li H-L, Lin R-Q, Zou F-C, Zhu X-Q and Chen J-X (2011) Genetic characterization, species differentiation and detection of *Fasciola* spp. by molecular approaches. *Parasites & Vectors* **4**(1), 101. https://doi.org/10.1186/1756-3305-4-101

Alba A, Vazquez AA and Hurtrez-boussès S (2021) Towards the comprehension of fasciolosis (re-)emergence: An integrative overview. *Parasitology* **148**(4), 385–407. https://doi.org/10.1017/s0031182020002255

Allen JE and Wynn TA (2011) Evolution of Th2 immunity: A rapid repair response to tissue destructive pathogens. *PLoS Pathogens* **7**(5), e1002003. https://doi.org/10.1371/journal.ppat.1002003

Altschul SF, Gish W, Miller W, Myers EW and Lipman DJ (1990) Basic local alignment search tool. *Journal of Molecular Biology* **215**(3), 403–410. https://doi.org/10.1016/s0022-2836(05)80360-2

Appleton CC and Miranda NAF (2015) Two Asian freshwater snails newly introduced into South Africa and an analysis of alien species reported to date. *African Invertebrates* **56**(1), 1–17,17.

Behm CA and Sangster NC (1999) Pathology, pathophysiology and clinical aspects. In Dalton JP (ed.), *Fasciolosis*. Wallingford: CABI Publishing, 185–217.

Bengis RG, Gakuya F, Munyeme M, Shiferaw DF, Kock RA and Chardonnet P (2023) Infections and parasites of free-ranging African Buffalo. In Caron A, Cornélis D, Chardonnet P and Prins HHT (eds.), *Ecology and Management of the African Buffalo*. Cambridge: Cambridge University Press, 239–268.

Blasco-Costa I, Cutmore SC, Miller TL and Nolan MJ (2016) Molecular approaches to trematode systematics: 'Best practice' and implications for future study. *Systematic Parasitology* **93**(3), 295–306. https://doi.org/10.1007/s11230-016-9631-2

Born-Torrijos A, Poulin R, Raga JA and Holzer AS (2014) Estimating trematode prevalence in snail hosts using a single-step duplex PCR: How badly does cercarial shedding underestimate infection rates? *Parasites & Vectors* **7**(1), 243. https://doi.org/10.1186/1756-3305-7-243

Brearley G, Rhodes J, Bradley A, Baxter G, Seabrook L, Lunney D, Liu Y and McAlpine C (2013) Wildlife disease prevalence in human-modified landscapes. *Biological Reviews* **88**(2), 427–442. https://doi.org/10.1111/brv.12009

Brecko J, Mathys A, Dekoninck W, Leponce M, VandenSpiegel D and Semal P (2014) Focus stacking: Comparing commercial top-end set-ups with a semi-automatic low budget approach. A possible solution for mass digitization of type specimens. *ZooKeys* **464**, 1–23.

Brooks DR (1988) Macroevolutionary comparisons of host and parasite phylogenies. *Annual Review of Ecology and Systematics* **19**(1), 235–259.

Brown DS (1994) *Freshwater Snails of Africa and Their Medical Importance*, 2nd edn. London: Taylor & Francis.

Brown DS and Kristensen TK (1989) *A Field Guide to African Freshwater Snails. 8. Southern African Species*. Charlottenlund: Danish Bilharziasis Laboratory.

Carlson CJ, Hopkins S, Bell KC, Dona J, Godfrey SS, Kwak ML, Lafferty KD, Moir ML, Speer KA, Strona G, Torchin M and Wood CL (2020) A global parasite conservation plan. *Biological Conservation* **250**, 108596. https://doi.org/10.1016/j.biocon.2020.108596

Carolus H, Muzarabani KC, Hammoud C, Schols R, Volckaert FAM, Barson M and Huyse T (2019) A cascade of biological invasions and parasite spillback in man-made Lake Kariba. *Science of the Total Environment* **659**, 1283–1292. https://doi.org/10.1016/j.scitotenv.2018.12.307

Catalano S, Nadler SA, Fall CB, Marsh KJ, Léger E, Sène M, Priestnall SL, Wood CL, Diouf ND, Bâ K and Webster JP (2019) *Plagiorchis* sp. in small mammals of Senegal and the potential emergence of a zoonotic trematodiasis. *International Journal Forest Parasitology: Parasites and Wildlife* **8**, 164–170. https://doi.org/10.1016/j.ijppaw.2019.02.003

Chai J-Y (2019) Plagiorchiids. *Human Intestinal Flukes: From Discovery to Treatment and Control* 463–489. Dordrecht: Springer Netherlands.

Chai J-Y, Cho J, Chang T, Jung B-K and Sohn W-M (2020) Taxonomy of *Echinostoma revolutum* and 37-Collar-Spined *Echinostoma* spp.: A Historical Review. *The Korean Journal of Parasitology* **58**(4), 343–371. https://doi.org/10.3347/kjp.2020.58.4.343

Chibwana F and Nkwengulila G (2019) A faunistic survey of digenean larvae infecting freshwater snails *Biomphalaria, Radix* and *Bulinus* species in the Lake Victoria and Mindu dam, Morogoro in Tanzania. *Tanzania Journal of Science* **43**, 1–13.

Chingwena G, Mukaratirwa S, Kristensen TK and Chimberi M (2002) Susceptibility of freshwater snails to the amphistome *Calicophoron microbothrium* and the influence of the species on susceptibility of *Bulinus tropicus* to *Schistosoma haematobium* and *Schistosoma mattheei* infections. *Journal of Parasitology* **88**(5), 880–883. https://doi.org/10.1645/0022-3395(2002)088[0880:Sofstt]2.0.Co;2

Cornelis D, Renaud PC, Melletti M, Fonteyn D, Bonhotal H, Hauptfleisch M, Asefa A, Breuer T, Korte L, Scholte P, Elkan P, Kohi E, Mwiu S, Ngene S, Omondi P, Tadjo SP, Prin T, Caron A, Prins HHT and Chardonnet P (2023) Conservation Status of the African Buffalo: A Continent-Wide Assessment. In Caron A, Cornélis D, Chardonnet P and Prins HHT (eds.), *Ecology and Management of the African Buffalo*. Cambridge: Cambridge University Press, 66–128.

Dar Y, Rondelaud D, Vignoles P and Dreyfuss G (2015) *Pseudosuccinea columella*: Age resistance to *Calicophoron daubneyi* infection in two snail populations. *Parasite (Paris, France)* **22**, 6.

DBL-WHO (1977) *A Field Guide to African Freshwater Snails. 4: South East African Species*. Charlottenlund: Danish Bilharziasis Laboratory.

DBL-WHO (1986) *A Field Guide to African Freshwater Snails 3. North East African Species*, 2nd Edition. Charlottenlund: Danish Bilharziasis Laboratory.

De Oliveira JB, Felix-nascimento G, Berenguer LKAR, Da Silva E Souza D, Bernal-valle S and De Souza VC (2024) Internal parasites and their impact on the health and conservation of neotropical vertebrates. In Acosta-jamett G and Chaves A (eds.), *Ecology of Wildlife Diseases in the Neotropics*. Cham: Springer International Publishing, 381–410.

Demann F and Wegner KM (2019) Infection by invasive parasites increases susceptibility of native hosts to secondary infection via modulation of cellular immunity. *Journal of Animal Ecology* **88**(3), 427–438. https://doi.org/10.1111/1365-2656.12939

Dinnik JA (1962) *Paramphistomum daubneyi* sp.nov. from cattle and its snail host in the Kenya Highlands. *Parasitology* **52**(1-2), 143–151.

Eduardo SL (1983) The taxonomy of the family Paramphistomidae Fischoeder, 1901 with special reference to the morphology of species occurring in ruminants. III. Revision of the genus *Calicophoron* Näsmark, 1937. *Systematic Parasitology* **5**(1), 25. https://doi.org/10.1007/bf00010983

Elelu N and Eisler MC (2018) A review of bovine fasciolosis and other trematode infections in Nigeria. *Journal of Helminthology* **92**(2), 128–141. https://doi.org/10.1017/S0022149X17000402

Engelstädter J and Fortuna NZ (2019) The dynamics of preferential host switching: Host phylogeny as a key predictor of parasite distribution*. *Evolution; International Journal of Organic Evolution* **73**(7), 1330–1340. https://doi.org/10.1111/evo.13716

Ezenwa VO and Jolles AE (2011) From host immunity to pathogen invasion: The effects of helminth coinfection on the dynamics of microparasites. *Integrative and Comparative Biology* **51**(4), 540–551. https://doi.org/10.1093/icb/icr058

Ezenwa VO and Jolles AE (2015) Opposite effects of anthelmintic treatment on microbial infection at individual versus population scales. *Science (New York, N.Y.)* **347**(6218), 175–177. https://doi.org/10.1126/science.1261714

Folmer O, Black M, Hoeh W, Lutz R and Vrijenhoek R (1994) DNA primers for amplification of mitochondrial cytochrome c oxidase subunit I from diverse metazoan invertebrates. *Molecular Marine Biology and Biotechnology* **3**(5), 294–299.

Frandsen F and Christensen NO (1984) An introductory guide to the identification of cercariae from African freshwater snails with special reference to cercariae of trematode species of medical and veterinary importance. *Acta Tropica* **41**(2), 181–202.

Ghatani S and Tandon V (2024) Amphistomes. In Toledo R and Fried B (eds.), *Digenetic Trematodes*. Cham: Springer International Publishing, 323–347.

Gillespie TR and Chapman CA (2008) Forest fragmentation, the decline of an endangered primate, and changes in host-parasite interactions relative to an unfragmented forest. *American Journal of Primatology* **70**(3), 222–230. https://doi.org/10.1002/ajp.20475

Gottdenker NL, Streicker DG, Faust CL and Carroll CR (2014) Anthropogenic land use change and infectious diseases: A review of the evidence. *Ecohealth* **11**(4), 619–632. https://doi.org/10.1007/s10393-014-0941-z

Grabner DS, Mohamed FAMM, Nachev M, Méabed EMH, Sabry AHA and Sures B (2014) Invasion biology meets parasitology: A case study of parasite spill-back with egyptian *Fasciola gigantica* in the invasive snail *Pseudosuccinea columella*. *Plos One* **9**(2), e88537. https://doi.org/10.1371/journal.pone.0088537

Grobler DG (1996) The potential utilization of the African Buffalo with regard to hunting and meat production. In Penzhorn BL (ed.), *The African Buffalo as a Game Ranch Animal*. Onderstepoort: South African Veterinary Association Wildlife Group, 37–42.

Guindon S, Dufayard J-F, Lefort V, Anisimova M, Hordijk W and Gascuel O (2010) New algorithms and methods to estimate maximum-likelihood phylogenies: Assessing the performance of PhyML 3.0. *Systematic Biology* **59**(3), 307–321, pmid = 20525638. https://doi.org/10.1093/sysbio/syq010

Hadebe MI, Manyangadze T, Kalinda C, Mindu T and Chimbari MJ (2023) Infection rates of *Fasciola* intermediate host snail species and their distribution in Africa: A systematic review and meta-analysis. *Tropical Medicine and Infectious Disease*. https://doi.org/10.3390/tropicalmed8100467

Hammoud C, Mulero S, Van Bocxlaer B, Boissier J, Verschuren D, Albrecht C and Huyse T (2022) Simultaneous genotyping of snails and infecting trematode parasites using high-throughput amplicon sequencing. *Molecular Ecology Resources* **22**(2), 567–586. https://doi.org/10.1111/1755-0998.13492

Hasegawa M, Kishino H and Yano T-A (1985) Dating of the human-ape splitting by a molecular clock of mitochondrial DNA. *Journal of Molecular Evolution* **22**(2), 160–174. https://doi.org/10.1007/BF02101694

Hoang Quang V, Levecke B, Dung DT, Binh VTL, Hien NTT, Ha NN, Thanh DTH, Devleesschauwer B, De Jong T, Paredis L, De Wilde N, Casaert S, Polman K, Callens S, Dorny P and Dermauw V (2026) Prevalence and risk factors related to *Fasciola* spp. transmission in north-Central Vietnam: A cross-sectional study in multiple host and environmental compartments. *One Health (Amsterdam, Netherlands)* **22**, 101417. https://doi.org/10.1016/j.onehlt.2026.101417

Howell AK, Tongue SC, Currie C, Evans J, Williams DJL and McNeilly TN (2018) Co-infection with *Fasciola hepatica* may increase the risk of *Escherichia coli* O157 shedding in British cattle destined for the food chain. *Preventive Veterinary Medicine* **150**, 70–76. https://doi.org/10.1016/j.prevetmed.2017.12.007

Huson KM, Oliver NAM and Robinson MW (2017) Paramphistomosis of ruminants: An emerging parasitic disease in Europe. *Trends in Parasitology* **33**(11), 836–844. https://doi.org/10.1016/j.pt.2017.07.002

Hutchinson GW, Dawson K, Fitzgibbon CC and Martin PJ (2009) Efficacy of an injectable combination anthelmintic (nitroxynil+clorsulon+ivermectin) against early immature *Fasciola hepatica* compared to triclabendazole combination flukicides given orally or topically to cattle. *Veterinary Parasitology* **162**(3-4), 278–284. https://doi.org/10.1016/j.vetpar.2009.03.032

IUCN SSC Antelope Specialist Group (2019) *Syncerus caffer*. The IUCN Red List of Threatened Species. https://dx.doi.org/10.2305/IUCN.UK.2019-1.RLTS.T21251A50195031.en

Johansen MV, Lier T and Sithithaworn P (2015) Towards improved diagnosis of neglected zoonotic trematodes using a one health approach. *Acta Tropica* **141**, 161–169. https://doi.org/10.1016/j.actatropica.2013.07.006

Jones BA, Grace D, Kock R, Alonso S, Rushton J, Said MY, McKeever D, Mutua F, Young J, McDermott J and Pfeiffer DU (2013) Zoonosis emergence linked to agricultural intensification and environmental change. *Proceedings of the National Academy of Sciences* **110**(21), 8399–8404. https://doi.org/10.1073/pnas.1208059110

Jones S, Juhász A, Makaula P, Cunningham LJ, Archer J, Nkolokosa C, Namacha G, Kambewa E, Lally D, Kapira DR, Chammudzi P, Kayuni SA, Musaya J and Stothard JR (2024) A first report of *Pseudosuccinea columella* (Say, 1817), an alien intermediate host for liver fluke, in Malawi. *Parasites & Vectors* **17**(1), 186. https://doi.org/10.1186/s13071-024-06241-5

Kamiya T, O'dwyer K, Nakagawa S and Poulin R (2014) Host diversity drives parasite diversity: Meta-analytical insights into patterns and causal mechanisms. *Ecography* **37**(7), 689–697. https://doi.org/10.1111/j.1600-0587.2013.00571.x

Kaplan RM, Dame JB, Reddy GR and Courtney CH (1995) A repetitive DNA probe for the sensitive detection of *Fasciola hepatica* infected snails. *International Journal for Parasitology* **25**(5), 601–610. https://doi.org/10.1016/0020-7519(94)00159-L

Katoh K, Misawa K, Kuma K and Miyata T (2002) MAFFT: A novel method for rapid multiple sequence alignment based on fast fourier transform. *Nucleic Acids Research* **30**(14), 3059–3066. https://doi.org/10.1093/nar/gkf436

Kiesecker JM (2002) Synergism between trematode infection and pesticide exposure: A link to amphibian limb deformities in nature? *Proceedings of the National Academy of Sciences of the United States of America* **99**(15), 9900–9904. https://doi.org/10.1073/pnas.152098899

Kock RA, Bengis RG, Shiferaw FD, Gakuya F, Mdetele D, Prins HHT, Caron A and Kock MD (2023) African buffalo and colonial cattle: Is 'systems change' the best future for farming and nature in Africa? In Caron A, Cornélis D, Chardonnet P and Prins HHT (eds.), *Ecology and Management of the African Buffalo*. Cambridge: Cambridge University Press, 320–350.

Kouadio JN, Giovanoli Evack J, Achi LY, Balmer O, Utzinger J, N'goran EK, Bonfoh B, Hattendorf J and Zinsstag J (2021) Efficacy of triclabendazole and albendazole against *Fasciola* spp. infection in cattle in Côte d'Ivoire: A randomised blinded trial. *Acta Tropica* **222**, 106039. https://doi.org/10.1016/j.actatropica.2021.106039

Krämer F and Schnieder T (1998) Sequence heterogeneity in a repetitive DNA element of *Fasciola*. *International Journal for Parasitology* **28**(12), 1923–1929. https://doi.org/10.1016/S0020-7519(98)00162-3

Kumar S, Stecher G, Li M, Knyaz C and Tamura K (2018) MEGA X: Molecular evolutionary genetics analysis across computing platforms. *Molecular Biology and Evolution* **35**(6), 1547–1549. https://doi.org/10.1093/molbev/msy096

Lafferty KD and Kuris AM (1999) How environmental stress affects the impacts of parasites. *Limnology and Oceanography* **44**(3part2), 925–931. https://doi.org/10.4319/lo.1999.44.3_part_2.0925

Laidemitt MR, Anderson LC, Wearing HJ, Mutuku MW, Mkoji GM and Loker ES (2019) Antagonism between parasites within snail hosts impacts the transmission of human schistosomiasis. *eLife* **8**, e50095. https://doi.org/10.7554/eLife.50095

Laidemitt MR, Zawadzki ET, Brant SV, Mutuku MW, Mkoji GM and Loker ES (2016) Loads of trematodes: Discovering hidden diversity of paramphistomoids in Kenyan ruminants. *Parasitology* **144**(2), 131–147. https://doi.org/10.1017/S0031182016001827

Lanfear R, Calcott B, Ho SYW and Guindon S (2012) PartitionFinder: Combined selection of partitioning schemes and substitution models for phylogenetic analyses. *Molecular Biology and Evolution* **29**(6), 1695–1701. https://doi.org/10.1093/molbev/mss020

Lanfear R, Frandsen PB, Wright AM, Senfeld T and Calcott B (2017) PartitionFinder 2: New methods for selecting partitioned models of evolution for molecular and morphological phylogenetic analyses. *Molecular Biology and Evolution* **34**(3), 772–773, pmid=28013191. https://doi.org/10.1093/molbev/msw260

Larsson A (2014) AliView: A fast and lightweight alignment viewer and editor for large datasets. *Bioinformatics (Oxford, England)* **30**(22), 3276–3278. https://doi.org/10.1093/bioinformatics/btu531

Lawton SP, Lim RM, Dukes JP, Kett SM, Cook RT, Walker AJ and Kirk RS (2015) Unravelling the riddle of *Radix*: DNA barcoding for species identification of freshwater snail intermediate hosts of zoonotic digeneans and estimating their inter-population evolutionary relationships. *Infection, Genetics and Evolution* **35**, 63–74. https://doi.org/10.1016/j.meegid.2015.07.021

Le Roex N, Cooper D, Van Helden PD, Hoal EG and Jolles AE (2016) Disease control in wildlife: Evaluating a test and cull programme for bovine tuberculosis in African Buffalo. *Transboundary and Emerging Diseases* **63**(6), 647–657. https://doi.org/10.1111/tbed.12329

Lemoine F, Correia D, Lefort V, Doppelt-azeroual O, Mareuil F, Cohen-boulakia S and Gascuel O (2019) NGPhylogeny.fr: New generation phylogenetic services for non-specialists. *Nucleic Acids Research* **47**(W1), W260–W265. https://doi.org/10.1093/nar/gkz303

LeSage KE and Fried B (2011) Encystment and excystment of the paramphistomid trematode *Zygocotyle lunata*. *Journal of Helminthology* **85**(3), 300–303. https://doi.org/10.1017/S0022149X10000593

Lounnas M, Correa AC, Vázquez AA, Dia A, Escobar JS, Nicot A, Arenas J, Ayaqui R, Dubois MP, Gimenez T, Gutiérrez A, González-ramírez C, Noya O, Prepelitchi L, Uribe N, Wisnivesky-colli C, Yong M, David P, Loker ES, Jarne P, Pointier JP and Hurtrez-boussès S (2017) Self-fertilization, long-distance flash invasion and biogeography shape the population structure of *Pseudosuccinea columella* at the worldwide scale. *Molecular Ecology* **26**(3), 887–903. https://doi.org/10.1111/mec.13984

Maddison WP and Maddison DR (2023) Mesquite: A modular system for evolutionary analysis. Version 3.5. https://www.mesquiteproject.org

Mahulu A, Clewing C, Stelbrink B, Chibwana FD, Tumwebaze I, Stothard JR and Albrecht C (2019) Cryptic intermediate snail host of the liver fluke *Fasciola hepatica* in Africa. *Parasites & Vectors* **12**(1). https://doi.org/10.1186/s13071-019-3825-9

Malatji MP and Mukaratirwa S (2020) Molecular detection of natural infection of *Lymnaea (Pseudosuccinea) columella* (Gastropoda: Lymnaeidae) with *Fasciola gigantica* (Digenea: Fasciolidae) from two provinces of South Africa. *Journal of Helminthology* **94**, e38. https://doi.org/10.1017/S0022149X19000129

Malatji MP, Pfukenyi DM and Mukaratirwa S (2020) *Fasciola* species and their vertebrate and snail intermediate hosts in East and Southern Africa: A review. *Journal of Helminthology* **94**, e63. https://doi.org/10.1017/S0022149X19000531

Mandahl-Barth G (1962) Key to the identification of east and Central African freshwater snails of medical and veterinary importance. *Bulletin of the World Health Organization* **27**(1), 135–150.

Marcogliese DJ and Pietrock M (2011) Combined effects of parasites and contaminants on animal health: Parasites do matter. *Trends in Parasitology* **27**(3), 123–130. https://doi.org/10.1016/j.pt.2010.11.002

McCully RM, Van Niekerk JW and Kruger SP (1967) Observations on the pathology of bilharziasis and other parasitic infestations of *Hippopotamus amphibius* Linnaeus, 1758, from the Kruger National Park. *Onderstepoort Journal of Veterinary Research* **34**(2), 563–617.

Mehmood K, Zhang H, Sabir AJ, Abbas RZ, Ijaz M, Durrani AZ, Saleem MH, Rehman MU, Iqbal MK, Wang YJ, Ahmad HI, Abbas T, Hussain R, Ghori MT, Ali S, Khan AU and Li JK (2017) A review on epidemiology, global prevalence and economical losses of fasciolosis in ruminants. *Microbial Pathogenesis* **109**, 253–262. https://doi.org/10.1016/j.micpath.2017.06.006

Miller MA, Pfeiffer W and Schwartz T (2010) Creating the CIPRES Science Gateway for inference of large phylogenetic trees. In *2010 Gateway Computing Environments Workshop (GCE)*.

Modabbernia G, Meshgi B and Kinsley AC (2024) Climatic variations and *Fasciola*: A review of impacts across the parasite life cycle. *Parasitology Research* **123**(8), 300. https://doi.org/10.1007/s00436-024-08319-6

Moreno MA, Holder M and Sukumaran J (2024) DendroPy 5: A mature Python library for phylogenetic computing. *Journal of Open Source Software* **9**(101), 6943. https://doi.org/10.21105/joss.06943

Morley NJ (2007) Anthropogenic effects of reservoir construction on the parasite fauna of aquatic wildlife. *Ecohealth* **4**(4), 374–383. https://doi.org/10.1007/s10393-007-0130-4

Mudavanhu A, Goossens E, Schols R, Manyangadze T, Nhiwatiwa T, Lemmens P, Huyse T and Brendonck L (2024a) Ecosystem links: Anthropogenic activities, environmental variables, and macrophytes structure snail preferences in man-made waterbodies. *Science of the Total Environment* **954**, 176394. https://doi.org/10.1016/j.scitotenv.2024.176394

Mudavanhu A, Schols R, Goossens E, Nhiwatiwa T, Manyangadze T, Brendonck L and Huyse T (2024b) One health monitoring reveals invasive freshwater snail species, new records, and undescribed parasite diversity in Zimbabwe. *Parasites & Vectors* **17**(1), 234. https://doi.org/10.1186/s13071-024-06307-4

Mueller RL (2006) Evolutionary rates, divergence dates, and the performance of mitochondrial genes in bayesian phylogenetic analysis. *Systematic Biology* **55**(2), 289–300. https://doi.org/10.1080/10635150500541672

Namirembe D, Huyse T, Wangalwa R, Tumusiime J and Tolo CU (2024) Liver fluke and schistosome cross-infection risk between livestock and wild mammals in Western Uganda, a one health approach. *International Journal Forest Parasitology: Parasites and Wildlife* **25**, 101022. https://doi.org/10.1016/j.ijppaw.2024.101022

Näsmark K (1937) A revision of the trematode family paramphistomidae. *Zoologiska Bidrag Fran Uppsala* **16**, 301–565.

Nukeri S, Malatji MP, Sengupta ME, Vennervald BJ, Stensgaard A-S, Chaisi M and Mukaratirwa S (2022) Potential hybridization of *Fasciola hepatica* and *F. gigantica* in Africa—A Scoping Review. *Pathogens (Basel, Switzerland)* **11**(11), 1303. https://doi.org/10.3390/pathogens11111303

Oppliger, Clobert, Lecomte, Lorenzon, Boudjemadi and John-alder (1998) Environmental stress increases the prevalence and intensity of blood parasite infection in the common lizard *Lacerta vivipara*. *Ecology Letters* **1**(2), 129–138. https://doi.org/10.1046/j.1461-0248.1998.00028.x

Outa J Omondi, Bhika P and Avenant-Oldewage A (2024) Gastropod invasions in anthropogenically impacted impoundments in South Africa: Tracing their origins and exploring field evidence of parasite spillback and amplification. *International Journal for Parasitology* **54**(6), 279–301. https://doi.org/10.1016/j.ijpara.2024.02.004

Pfukenyi DM, Mukaratirwa P, Willingham AL and Monrad J (2006) Epidemiological studies of *Fasciola gigantica* infections in cattle in the highveld and lowveld communal grazing areas of Zimbabwe. *Onderstepoort Journal of Veterinary Research* **73**(1), 15. https://doi.org/10.4102/ojvr.v73i1.168

Pfukenyi DM and Mukaratirwa S (2018) Amphistome infections in domestic and wild ruminants in East and Southern Africa: A review. *Onderstepoort Journal of Veterinary Research* **85**(1). https://doi.org/10.4102/ojvr.v85i1.1584

Pirotta E, Thomas L, Costa DP, Hall AJ, Harris CM, Harwood J, Kraus SD, Miller PJO, Moore MJ, Photopoulou T, Rolland RM, Schwacke L, Simmons SE, Southall BL and Tyack PL (2022) Understanding the combined effects of multiple stressors: A new perspective on a longstanding challenge. *Science of the Total Environment* **821**, 153322. https://doi.org/10.1016/j.scitotenv.2022.153322

Posada D (2003) Using MODELTEST and PAUP* to select a model of nucleotide substitution *Current Protocols in Bioinformatics*. (1). **Chapter 6**, Unit 6.5. https://doi.org/10.1002/0471250953.bi0605s00.

Price PW, Westoby M, Rice B, Atsatt PR, Fritz RS, Thompson JN and Mobley K (1986) Parasite mediation in ecological interactions. *Annual Review of Ecology, Evolution, and Systematics* **17**(1), 487–505. https://doi.org/10.1146/annurev.es.17.110186.002415

Prins HHT, Ottenburghs J and Hooft P (2023) The environments of the African buffalo, with different selection forces in different habitats. In Caron A, Cornélis D, Chardonnet P and Prins HHT (eds.), *Ecology and Management of the African Buffalo*. Cambridge: Cambridge University Press, 205–234.

Rambaut A, Drummond AJ, Xie D, Baele G and Suchard MA (2018) Posterior summarization in bayesian phylogenetics using tracer 1.7. *Systematic Biology* **67**(5), 901–904. https://doi.org/10.1093/sysbio/syy032

Rodríguez F, Oliver JL, Marín A and Medina JR (1990) The general stochastic model of nucleotide substitution. *Journal of Theoretical Biology* **142**(4), 485–501. https://doi.org/10.1016/S0022-5193(05)80104-3

Ronquist F, Teslenko M, Van der Mark P, Ayres DL, Darling A, Hhna S, Larget B, Liu L, Suchard MA and Huelsenbeck JP (2012) MrBayes 3.2: Efficient Bayesian phylogenetic inference and model choice across a large model space. *Systematic Biology* **61**(3), 539–542,pmid=22357727. https://doi.org/10.1093/sysbio/sys029

Schall JJ (1992) Parasite-mediated competition in *Anolis* lizards. *Oecologia* **92**(1), 58–64. https://doi.org/10.1007/BF00317262

Schols R, Carolus H, Hammoud C, Muzarabani KC, Barson M and Huyse T (2021) Invasive snails, parasite spillback, and potential parasite spillover drive parasitic diseases of *Hippopotamus amphibius* in artificial lakes of Zimbabwe. *BMC Biology* **19**(1), 160. https://doi.org/10.1186/s12915-021-01093-2

Schols R, Henrard A, Brecko J, Mudavanhu A, Goossens E, Steffanie N, Clegg S, Vanhove MPM and Huyse T (2025) Innovating stomach fluke identification: An integrative approach combining Micro-CT imaging and molecular tools. *International Journal for Parasitology* **55**(12), 615–630. https://doi.org/10.1016/j.ijpara.2025.05.002

Schols R and Huyse T (2024) Fasciola nyanzae. *Trends in Parasitology* **40**(6), 527–528. https://doi.org/10.1016/j.pt.2024.01.007

Schols R, Mudavanhu A, Carolus H, Hammoud C, Muzarabani KC, Barson M and Huyse T (2020) Exposing the barcoding void: An integrative approach to study snail-borne parasites in a one health context. *Frontiers in Veterinary Science* **7**, 605280. https://doi.org/10.3389/fvets.2020.605280

Schwelm J, Soldánová M, Vyhlídalová T, Sures B and Selbach C (2018) Small but diverse: Larval trematode communities in the small freshwater planorbids *Gyraulus albus* and *Segmentina nitida* (Gastropoda: Pulmonata) from the Ruhr River, Germany. *Parasitology Research* **117**(1), 241–255. https://doi.org/10.1007/s00436-017-5699-0

Sey O (1991) *CRC Handbook of the Zoology of Amphistomes (1st Ed.)*. Boca Raton: CRC Press.

Sibula MS, Malatji MP, Nyahunda C and Mukaratirwa S (2024a) Amphistome infection and species diversity of freshwater snails collected from selected wildlife drinking water sources in matebeleland region of zimbabwe. *Veterinary Sciences* **11**(5), 211.

Sibula MS, Nyagura I, Malatji MP and Mukaratirwa S (2024b) Prevalence and geographical distribution of amphistomes of African wild ruminants: A scoping review. *International Journal Forest Parasitology: Parasites and Wildlife* **23**. https://doi.org/10.1016/j.ijppaw.2024.100906

Simonis MC, Ciarrachi S, Dyer KE, Allira M, Demory B, Zubayr J, Van Parys D, Whitmore K, Fitzgerald K, Castle KT, Dewey TA, O'keefe JM, Bernard RF, Chumchal MM, Haase CG, Foster JT and Becker DJ (2025) A collaborative multiple stressor approach for identifying spatial heterogeneities in wildlife health and conservation priorities. *Integrative and Comparative Biology* **65**(6), 1772–1780. https://doi.org/10.1093/icb/icaf123

Soliman O, Montaser MM, Ashour AA, Soliman MI and Nigm AH (2019) SEM and molecular approaches to identify *Calicophoron clavula* in Saudi Arabia. *Journal of Parasitic Diseases* **44**(1), 239–247. https://doi.org/10.1007/s12639-019-01187-3

Sousa WP (2015) Interspecific interactions among larval trematode parasites of freshwater and marine snails. *American Zoologist* **32**(4), 583–592. https://doi.org/10.1093/icb/32.4.583

Sow S, De Vlas SJ, Engels D and Gryseels B (2002) Water-related disease patterns before and after the construction of the Diama dam in northern Senegal. *Annals of Tropical Medicine & Parasitology* **96**(6), 575–586. https://doi.org/10.1179/000349802125001636

Sures B, Nachev M, Schwelm J, Grabner D and Selbach C (2023) Environmental parasitology: Stressor effects on aquatic parasites. *Trends in Parasitology* **39**(6), 461–474. https://doi.org/10.1016/j.pt.2023.03.005

Tamura K, Stecher G and Kumar S (2021) MEGA11: Molecular evolutionary genetics analysis version 11. *Molecular Biology and Evolution* **38**(7), 3022–3027. https://doi.org/10.1093/molbev/msab120

Taylor R, Bennitt E, Fynn R, Korte L, Naidoo R, Roug A and Cornelis D (2023) Habitat, space use and feeding ecology of the African Buffalo. In Caron A, Cornélis D, Chardonnet P and Prins HHT (eds.), *Ecology and Management of the African Buffalo*. Cambridge: Cambridge University Press, 133–152.

Telfer S and Bown K (2012) The effects of invasion on parasite dynamics and communities. *Functional Ecology* **26**(6). https://doi.org/10.1111/j.1365-2435.2012.02049.x

Thompson RCA (2013) Parasite zoonoses and wildlife: One health, spillover and human activity. *International Journal for Parasitology* **43**(12-13), 1079–1088. https://doi.org/10.1016/j.ijpara.2013.06.007

Toledo R and Fried B (2019) *Digenetic Trematodes*.

Tompkins DM, White AR and Boots M (2003) Ecological replacement of native red squirrels by invasive greys driven by disease. *Ecology Letters* **6**(3), 189–196. https://doi.org/10.1046/j.1461-0248.2003.00417.x

Vicente-Santos A, Willink B, Nowak K, Civitello DJ and Gillespie TR (2023) Host-pathogen interactions under pressure: A review and meta-analysis of stress-mediated effects on disease dynamics. *Ecology Letters* **26**(11), 2003–2020. https://doi.org/10.1111/ele.14319

Vilas R, Criscione CD and Blouin MS (2005) A comparison between mitochondrial DNA and the ribosomal internal transcribed regions in prospecting for cryptic species of platyhelminth parasites. *Parasitology* **131**(6), 839–846. https://doi.org/10.1017/S0031182005008437

Vítovec J, Kotrlá B, Haji H and Hayles LB (1984) Fatal infection of an elephant calf caused by the trematode *Protofasciola robusta* (Lorenz, 1881) in Somaliland. *Zentralblatt Für Veterinärmedizin Reihe B* **31**(1-10), 597–602. https://doi.org/10.1111/j.1439-0450.1984.tb01340.x

White TJ, Bruns TD, Lee SB and Taylor JW (1990) *Amplification and Direct Sequencing of Fungal Ribosomal RNA Genes for Phylogenetics. In PCR - Protocols and Applications - A Laboratory Manual*. San Diego: Academic Press. 315–322.

Woodburn DB, Steyl J, Du Plessis EC, Last RD, Reininghaus B and Mitchell EP (2021) Pathological findings in African buffaloes (*Syncerus caffer*) in South Africa. *Journal of the South African Veterinary Association* **92**(0), e1–e11. https://doi.org/10.4102/jsava.v92i0.2117

Xia X (2018) DAMBE7: New and improved tools for data analysis in molecular biology and evolution. *Molecular Biology and Evolution* **35**(6), 1550–1552. https://doi.org/10.1093/molbev/msy073

Zietara MS, Arndt A, Geets A, Hellemans B and Volckaert FA (2000) The nuclear rDNA region of *Gyrodactylus arcuatus* and *G. branchicus* (Monogenea: Gyrodactylidae). *Journal of Parasitology* **86**(6), 1368–1373. https://doi.org/10.1645/0022-3395(2000)086[1368:Tnrrog]2.0.Co;2

Zwickl D (2006) Genetic Algorithm Approaches for the Phylogenetic Analysis of Large Biological Sequence Datasets Under the Maximum Likelihood Criterion.